

1 **Modernizing the open-source community Noah-MP land surface model (version 5.0) with**  
2 **enhanced modularity, interoperability, and applicability**

3  
4 Cenlin He<sup>1</sup>, Prasanth Valayamkunnath<sup>1,5</sup>, Michael Barlage<sup>2</sup>, Fei Chen<sup>1</sup>, David Gochis<sup>1</sup>, Ryan  
5 Cabell<sup>1</sup>, Tim Schneider<sup>1</sup>, Roy Rasmussen<sup>1</sup>, Guo-Yue Niu<sup>3</sup>, Zong-Liang Yang<sup>4</sup>, Dev Niyogi<sup>4</sup>,  
6 Michael Ek<sup>1</sup>

7  
8 <sup>1</sup>National Center for Atmospheric Research (NCAR), Boulder, Colorado, USA

9 <sup>2</sup>NOAA Environmental Modeling Center (EMC), College Park, Maryland, USA

10 <sup>3</sup>University of Arizona, Tucson, Arizona, USA

11 <sup>4</sup>University of Texas Austin, Austin, Texas, USA

12 <sup>5</sup>Indian Institute of Science Education and Research Thiruvananthapuram, India

13

14

15 *Correspondence to:* Cenlin He (cenlinhe@ucar.edu)

16

17

18

19 **Abstract**

20

21 The widely-used open-source community Noah-MP land surface model (LSM) is designed for  
22 applications ranging from uncoupled land-surface and ecohydrological process studies to coupled  
23 numerical weather prediction and decadal global/regional climate simulations. It has been used in  
24 many coupled community weather/climate/hydrology models. In this study, we  
25 modernize/refactor the Noah-MP LSM by adopting modern Fortran code and data structures and  
26 standards, which substantially enhances the model modularity, interoperability, and applicability.  
27 The modernized Noah-MP is released as the version 5.0 (v5.0), which has five key features: (1)  
28 enhanced modularization and interoperability by re-organizing model physics into individual  
29 process-level Fortran module files, (2) enhanced data structure with new hierarchical data types  
30 and optimized variable declaration and initialization structures, (3) enhanced code structure and  
31 calling workflow by leveraging the new data structure and modularization, (4) enhanced  
32 (descriptive and self-explanatory) model variable naming standard, and (5) enhanced driver and  
33 interface structures to couple with host weather/climate/hydrology models. In addition, we create  
34 a comprehensive technical documentation of the Noah-MP v5.0 and a set of model benchmark and  
35 reference datasets. The Noah-MP v5.0 will be coupled to various weather/climate/hydrology  
36 models in the future. Overall, the modernized Noah-MP will allow a more efficient and convenient  
37 process for future model developments and applications.

38

39

40

## 41 1. Introduction

42

43 Land surface models (LSMs) are useful modeling tools to resolve terrestrial responses to and  
44 interactions with the atmosphere, ocean, glacier, and sea ice in the earth system. Traditionally,  
45 LSMs were thought to mainly provide lower boundary conditions to the coupled atmospheric  
46 models. However, modern LSMs have been increasingly employed as an indispensable component  
47 in the climate and weather systems to offer biogeophysical and biogeochemical insight for  
48 understanding and quantifying the impact and evolution of climate, weather, and the integrated  
49 earth environment (Blyth et al., 2021). LSMs have been widely applied to tackle many important  
50 societally relevant challenges, such as drought, flood, heat wave, water availability, agriculture,  
51 food security, wildfires, deforestation, and urbanization (Bonan and Doney, 2018).

52

53 Among many LSMs that have been developed in the past few decades, the open-source community  
54 Noah with Multi-parameterization Options (Noah-MP; Niu et al., 2011; Yang et al., 2011) is one  
55 of the most widely-used state-of-the-art LSMs. The article describing the Noah-MP model by Niu  
56 et al (2011) is *de facto* the most cited LSM paper in the last 10 years, highlighting its worldwide  
57 popular usage in the international science community. Compared to its predecessor, the Noah LSM  
58 (Chen et al., 1996, 1997; Chen and Dudhia, 2001; Ek et al., 2003), Noah-MP significantly  
59 improves known Noah limitations by employing enhanced treatments of vegetation canopy,  
60 snowpack, soil processes, groundwater, and their complex interactions as well as additional  
61 capabilities for critical land processes (e.g., crop, irrigation, tile drainage, groundwater, urban,  
62 carbon and nitrogen cycles). Another unique feature of Noah-MP is the inclusion of multiple  
63 physics options for different land processes, which allows the multi-physics model ensemble  
64 experiments for uncertainty assessment and testing competing hypotheses (Zhang et al., 2016; J.  
65 Li et al., 2020).

66

67 Noah-MP can be applied to various spatial scales spanning from point scale locally to ~100-km  
68 resolution globally, and temporal scales spanning from sub-daily to decadal time scales. Since its  
69 original development, Noah-MP has been used in many important applications, including  
70 numerical weather prediction (Suzuki and Zupanski, 2018; Ju et al., 2022), high-resolution climate  
71 modeling (Gao et al., 2017; Liu et al., 2017; Rasmussen et al., 2023), land data assimilation (Xu  
72 et al., 2021; Nie et al., 2022), drought (Arsenault et al., 2020; Niu et al., 2020; Wu et al., 2021;  
73 Abolafia-Rosenzweig et al., 2023a), wildfire (Kumar et al., 2021; Abolafia-Rosenzweig et al.,  
74 2022a, 2023b), snowpack evolution (Wrzesien et al., 2015; He et al., 2019; Jiang et al., 2020),  
75 hydrology and water resources (Cai et al., 2014; Liang et al., 2019; X. Zhang et al., 2022a; Hazra  
76 et al., 2023), crop and agricultural management (Liu et al., 2016; Ingwersen et al., 2018; Warrach-  
77 Sagi et al., 2022; Valayamkunnath et al., 2022; Zhang et al., 2020, 2023), urbanization and heat  
78 island (Xu et al., 2018; Salamanca et al., 2018; Patel et al., 2022), biogeochemical cycle (Cai et  
79 al., 2016; Brunsell et al., 2021), wind erosion (Jiang et al., 2021), wetland (Z. Zhang et al., 2022),  
80 groundwater (Barlage et al., 2015, 2021; Li et al., 2022), and landslide hazard (Zhuo et al., 2019).

81  
82 Currently, Noah-MP has been implemented into many community research and operational  
83 weather/climate/hydrology models, including the Weather Research and Forecasting model  
84 (WRF), the Model for Prediction Across Scales (MPAS), the NOAA operational National Water  
85 Model (NWM), the NOAA Unified Forecast System (UFS), the NASA Land Information System  
86 (LIS), and the NCAR High-Resolution Land Data Assimilation System (HRLDAS).

87  
88 Despite its popular usage in the international research and application communities, the Noah-MP  
89 core code engine was designed 12 years ago and is outdated, and does not take advantage of  
90 modern Fortran language architecture. It has a single lengthy (>12,000 lines) Fortran source file  
91 lumping together all model physics with complex code and data structures using inconsistent  
92 format and does not follow the modern Fortran code standard. This makes the Noah-MP model  
93 code difficult for users and developers to read, modify, and test as well as to implement and apply  
94 it to other community models. Furthermore, a lengthy code is error prone and challenging to debug.  
95 These issues limit the further development and application of Noah-MP.

96  
97 Therefore, this study is motivated to modernize (refactor) the entire Noah-MP model by adopting  
98 modern Fortran code and data structures and standards, which substantially enhances the model  
99 modularity, interoperability, and applicability. The base code used for refactoring is the Noah-MP  
100 version 4.5 (released in December 2022; [https://github.com/NCAR/noahmp/tree/release-v4.5-](https://github.com/NCAR/noahmp/tree/release-v4.5-WRF)  
101 [WRF](https://github.com/NCAR/noahmp/tree/release-v4.5-WRF)), and the refactoring effort does not change model physics. We release the  
102 modernized/refactored Noah-MP as version 5.0 (v5.0; <https://github.com/NCAR/noahmp>), which  
103 includes five key features: (1) enhanced modularization and interoperability by re-organizing  
104 model physics into individual process-level Fortran module files, (2) enhanced data structure with  
105 new hierarchical data types and optimized variable declaration and initialization structures, (3)  
106 enhanced code structure and subroutine calling workflow by leveraging the new data structure and  
107 modularization and refining code to be more concise, (4) enhanced (descriptive and self-  
108 explanatory) model variable naming standard, and (5) enhanced driver and interface code  
109 structures to couple with host weather/climate/hydrology models. In addition, we have created a  
110 comprehensive technical documentation (He et al., 2023) to describe model physics and details of  
111 the refactored Noah-MP and a set of model benchmark and reference datasets for future  
112 comparison and assessment. Overall, the modernized open-source community Noah-MP model  
113 (version 5.0) will allow a more efficient and convenient process for future model developments  
114 and applications. The framework and practice in the course of refactoring the entire Noah-MP code  
115 is also applicable to other LSMs and ESMs.

116  
117 This paper reports the key features of the modernized Noah-MP v5.0 and is organized as follows.  
118 Section 2 briefly summarizes the Noah-MP model physics with several updates since its original  
119 development. Sections 3–7, respectively, introduce the key features of the modernized Noah-MP  
120 in terms of enhanced model modularization, data type, code structure, variable naming, and

121 coupling structure with host models. Section 8 describes the model benchmarking and reference  
122 datasets. Section 9 provides the release information of model code and technical documentation.  
123 Section 10 concludes the paper with future model development plans.

124

## 125 **2. Noah-MP version 5.0 model physics**

126

### 127 **2.1 Noah-MP description**

128

129 Noah-MP (Niu et al., 2011) was originally developed based on the Noah LSM (Chen et al., 1996,  
130 1997; Chen and Dudhia, 2001; Ek et al., 2003) to augment its modeling capabilities with enhanced  
131 physical representations and treatments of dynamic vegetation, canopy interception and radiative  
132 transfer processes, multi-layer snowpack physics, and soil and hydrological processes. The history  
133 of model development and evolution has been described in the technical documentation (He et al.,  
134 2023). Noah-MP is designed to simulate land surface and subsurface energy and water processes  
135 in both uncoupled and coupled modes with atmospheric or hydrological models at sub-daily time  
136 scale and high spatial resolution (even for point scale). This further allows the use of Noah-MP in  
137 different hydrological, weather, and climate models for applications in a wide range of spatial and  
138 temporal scales with proper integration in time and space.

139

140 Noah-MP divides its land grid into two sub-grid tiles, namely vegetated and non-vegetated grounds,  
141 based on vegetation cover fraction. The biogeophysical and biogeochemical processes are treated  
142 separately for the vegetated and bare grounds. Noah-MP adopts a “big-leaf” canopy treatment  
143 characterized by canopy properties dependent on vegetation types. Noah-MP accounts for a  
144 multiple-layer snowpack, where snow ice and liquid water content, density, depth, and temperature  
145 are simulated dynamically. Noah-MP also includes multi-layer soil thermal and hydrological  
146 processes with dynamically evolving soil temperature and water content. The vegetation, snow,  
147 and soil components in Noah-MP are closely coupled and interacted with each other via complex  
148 energy, water, and biochemical processes. Their detailed physical formulations and  
149 parameterizations in Noah-MP v5.0 are described in the technical documentation (He et al., 2023).  
150 Below, we briefly summarize the energy, water, and biochemical processes in Noah-MP v5.0.

151

### 152 **2.2 Noah-MP energy processes**

153

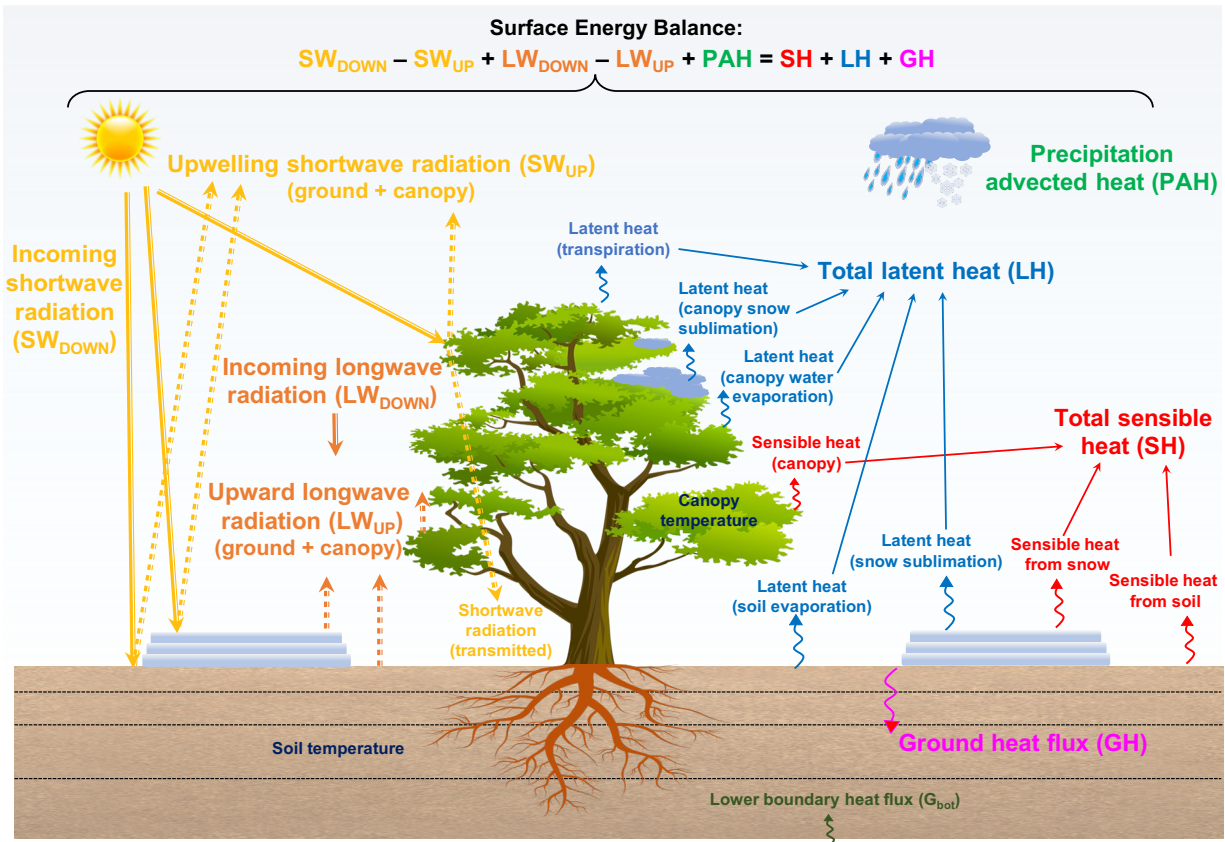
154 Noah-MP resolves energy budgets and processes separately for vegetated and non-vegetated  
155 ground portions of each grid (Niu et al., 2011). The vegetation cover fraction, either from  
156 observational inputs or model calculations based on leaf area index (LAI) inputs or predicted by  
157 the dynamic vegetation module, is used to separate vegetated and bare grounds. The grid-mean  
158 energy states and fluxes are calculated as an average of vegetated and bare ground values weighted  
159 by vegetation cover fraction. For surface radiative processes driven by incoming shortwave and  
160 longwave radiation (atmospheric forcing), Noah-MP simulates the radiative absorption and

161 scattering by the canopy and ground (soil/snow) as well as the longwave emissions by the canopy  
162 and ground (soil/snow). The net absorbed total (shortwave and longwave) radiative flux is  
163 balanced by precipitation advected heat flux, total surface sensible and latent heat fluxes, and  
164 ground heat flux. The precipitation advected heat flux represents the heat flux advected from  
165 precipitation (rain/snow) to canopy/ground due to the temperature difference between precipitation  
166 (surface air) and canopy/ground. The total surface sensible heat includes the sensible heat from  
167 canopy, snowpack, and soil surfaces. The total surface latent heat includes the latent heat from  
168 snowpack sublimation, soil evaporation, canopy snow sublimation, canopy water evaporation, and  
169 plant transpiration. The ground heat flux is the heat flux leaving the ground surface to drive  
170 subsurface snow/soil phase change and/or temperature changes.

171  
172 To model the aforementioned surface energy flux components, Noah-MP dynamically calculates  
173 a number of key land surface properties, include ground snow cover fraction, surface roughness,  
174 canopy and ground thermal properties, snow and soil albedo, surface emissivity, and canopy  
175 radiative transfer. Many of these property and process calculations have multiple physics options  
176 (see Sect. 2.6). Based on the canopy and ground energy balance, Noah-MP further solves the  
177 temperature and phase change for canopy, snowpack, and soil. Figure 1 summarizes the key energy  
178 processes and budget components as well as the energy balance equation in Noah-MP v5.0. Note  
179 that the energy processes at glacier grids are treated similarly to those at 100% bare (non-vegetated)  
180 ground grids except that the soil is replaced by glacier ice with ice-specific properties.

181

## Noah-MP Energy Budget and Processes



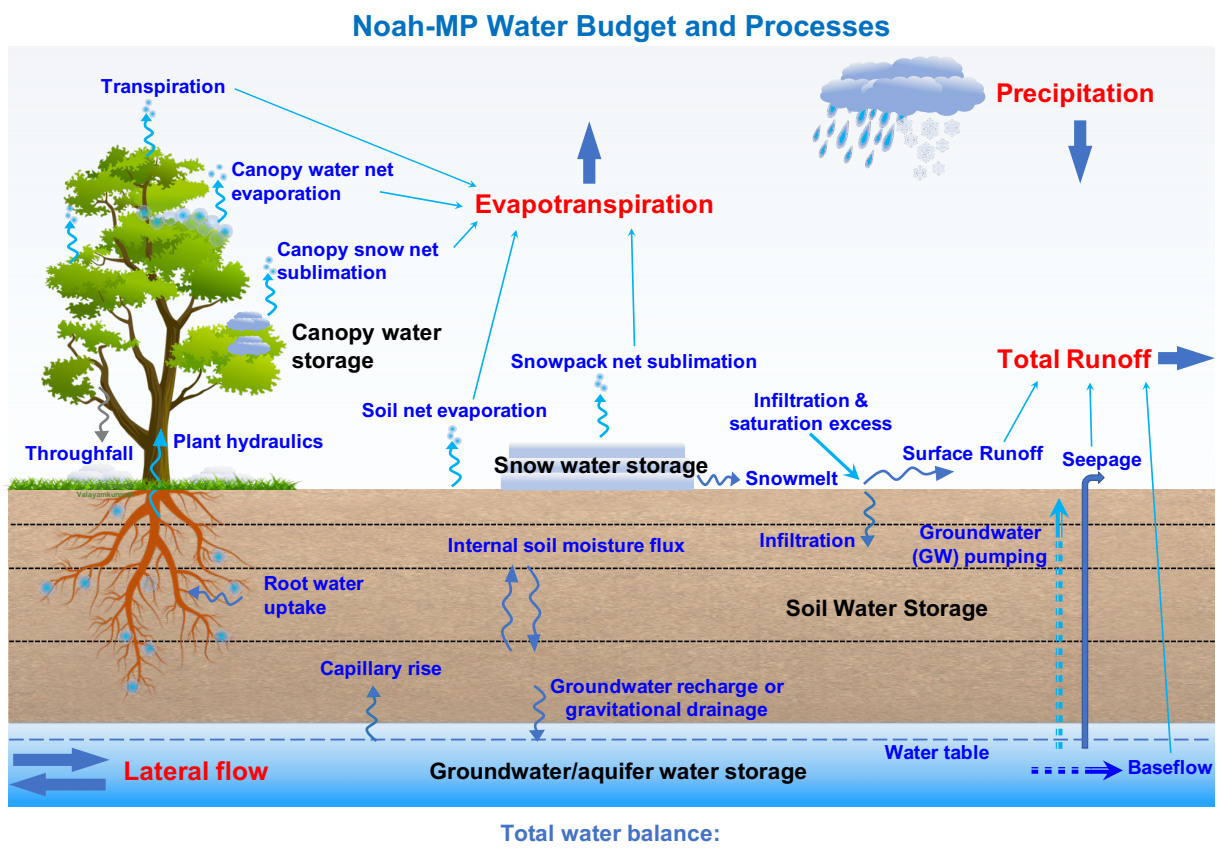
182  
 183 **Figure 1.** Schematic diagram of energy budget and processes represented in Noah-MP version 5.0.  
 184

185  
 186

### 2.3 Noah-MP water processes

187  
 188 Noah-MP accounts for five major water budget components, including precipitation,  
 189 evapotranspiration (ET), total runoff, net lateral flow, and total water storage change intercepted  
 190 by the canopy and in snow, soil, and aquifer. For precipitation, Noah-MP has several temperature-  
 191 based rainfall-snowfall partitioning parameterizations or can use the partitioning from atmospheric  
 192 models directly (see Sect. 2.6). Noah-MP simulates canopy interception and throughfall of rain  
 193 and snow, where the intercepted rain and snow on the canopy can go through unloading/dripping,  
 194 frost, sublimation, melting, and freezing processes. Net evaporation loss from the canopy-  
 195 intercepted liquid water (evaporation minus dew), net sublimation from the canopy-intercepted  
 196 snow (sublimation minus frost), transpiration (via plant hydraulics), net soil surface evaporation,  
 197 and net snowpack sublimation together contribute to the total surface ET. Noah-MP dynamically  
 198 simulates multi-layer snowpack water storage (ice and liquid water) changes driven by  
 199 snowfall/rainfall, frost, sublimation, freezing, and melting. The snowmelt water out of snowpack  
 200 together with rainfall at the soil surface are further partitioned into surface runoff and infiltration  
 201 based on multiple runoff and infiltration physics options (see Sect. 2.6). Soil moisture and

202 unsaturated water flow across soil layers are simulated using the one-dimensional Richards  
 203 equation. Two optional groundwater schemes, one without 2-D lateral flow (Niu et al., 2007) and  
 204 one with 2-D lateral flow (Fan et al., 2007; Miguez-Macho et al. 2007), are available in Noah-MP  
 205 to simulate groundwater dynamics, including groundwater recharge, water table change, baseflow,  
 206 seepage, and/or lateral flow. Noah-MP also includes dynamic irrigation and tile drainage processes  
 207 for agricultural management applications (Valayamkunnath et al., 2021, 2022). Figure 2  
 208 summarizes the key water processes and budget components as well as the water balance equation  
 209 in Noah-MP v5.0. Note that the water processes at glacier grids are treated similarly to those at  
 210 100% bare ground grids except that all the soil and subsurface hydrological processes are removed  
 211 and replaced by glacier ice (He et al., 2023).  
 212



**Precipitation + lateral flow – Evapotranspiration – Total Runoff = Δ (water storage in canopy, snow, soil, aquifer)**

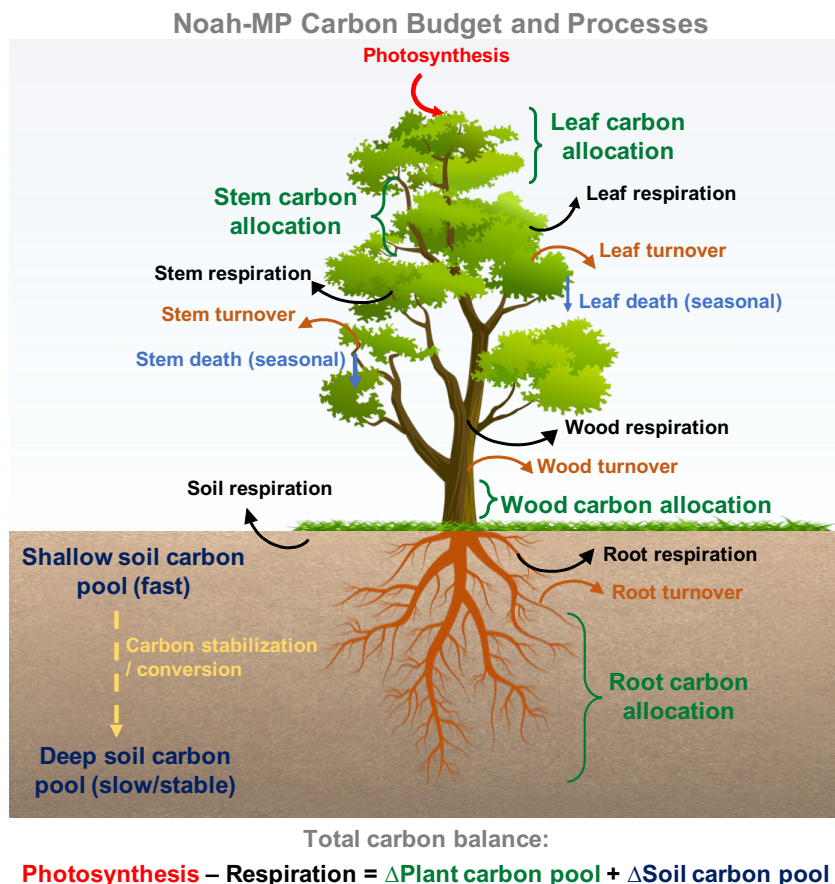
213  
 214 **Figure 2.** Schematic diagram of water budget and processes represented in Noah-MP version 5.0.  
 215

216  
 217 **2.4 Noah-MP biochemical processes**  
 218

219 Currently, the community version of Noah-MP only accounts for carbon processes for biochemical  
 220 cycles, while nitrogen dynamics and soil carbon dynamics have been developed in non-community  
 221 Noah-MP versions managed by individual research groups (e.g., Cai et al., 2016; X. Zhang et al.,



222 2022b). We will synthesize and integrate individual Noah-MP updates into the community version  
 223 in the future (see Sect. 2.5 for more discussions). Noah-MP simulates carbon processes for both  
 224 natural/generic vegetation (Niu et al., 2011) and explicit agricultural crops (Liu et al., 2016). The  
 225 carbon processes related to vegetation growth dynamics include (1) carbon assimilation from  
 226 photosynthesis by shaded and sunlit leaves, (2) carbon allocation to different parts of vegetation  
 227 (leaf, stem, wood and root) and soil carbon pools (fast and slow carbon), (3) carbon loss due to  
 228 respiration of different vegetation and soil carbon pools, (4) carbon transfer between vegetation  
 229 and fast soil carbon pools through vegetation (leaf, stem, wood and root) turnover and seasonal  
 230 death of leaf and stem, and (5) soil carbon pool conversion through soil carbon stabilization. The  
 231 total carbon flux to the atmosphere and net primary productivity are computed based on the  
 232 aforementioned carbon processes. Figure 3 summarizes the key carbon processes and budget  
 233 components as well as the carbon balance equation in Noah-MP v5.0. Note that the carbon  
 234 processes for crop growth are treated similarly to those of natural vegetation, except that the wood  
 235 component of plants is removed and the grain component of crops is added with additional carbon  
 236 conversion from leaf, stem, and root to grain depending on crop growing stages.  
 237



238 **Figure 3.** Schematic diagram of carbon budget and processes represented in Noah-MP version 5.0.  
 239  
 240  
 241



## 242 **2.5 Noah-MP physics updates since original development**

243

244 Since the release of the original Noah-MP in year 2011 (Niu et al., 2011), there are several  
245 important updates in Noah-MP physics. Some of the updates have been included in the community  
246 version of Noah-MP v5.0, while some are only available in the non-community versions managed  
247 by individual research groups. We will make efforts to synthesize and integrate individual Noah-  
248 MP updates into the community version in the future by working with those developer teams. Here,  
249 to the best of our knowledge, we briefly list the major Noah-MP physics updates from the  
250 community in the past decade.

251

252 The new/enhanced physics included in the community Noah-MP version 5.0 since 2011 are: (1)  
253 the Miguez-Macho-Fan (MMF) groundwater scheme (Barlage et al., 2015); (2) three additional  
254 runoff schemes: the Variable infiltration capacity (VIC), dynamic VIC, and Xinanjiang schemes  
255 (McDaniel et al., 2020); (3) tile drainage schemes (Valayamkunnath et al., 2022); (4) dynamic  
256 irrigation schemes (sprinkler, micro, and flooding irrigation) (Valayamkunnath et al., 2021); (5) a  
257 dynamic crop growth model for corn and soybean (Liu et al., 2016) with enhanced C3 and C4 crop  
258 parameters (Zhang et al., 2020); (6) coupling with urban canopy models (Xu et al., 2018;  
259 Salamanca et al., 2018) with local climate zone modeling capabilities (Zonato et al., 2021); (7)  
260 enhanced snow cover, snow compaction, and wind-canopy absorption parameters (He et al., 2021);  
261 (8) a wet-bulb temperature-based snow-rain partitioning scheme (Wang et al., 2019).

262

263 The new/enhanced physics currently not included in the community Noah-MP version 5.0 since  
264 2011 are: (1) nitrogen dynamics (Cai et al., 2016); (2) big-tree plant hydraulics (Li et al., 2021);  
265 (3) dynamic root optimization (Wang et al. 2018) with an explicit representation of plant water  
266 storage (Niu et al., 2020); (4) additional snow cover parameterizations (Jiang et al., 2020); (5)  
267 coupling with a wind erosion model (Jiang et al., 2021); (6) a wetland representation and dynamics  
268 (Z. Zhang et al., 2022); (7) a unified turbulence parameterization throughout the canopy and  
269 roughness sublayer (Abolafia-Rosenzweig et al., 2021); (8) enhanced snow albedo representations  
270 (Abolafia-Rosenzweig et al., 2022b); (9) coupling with a snow radiative transfer (SNICAR) model  
271 (Wang et al., 2020, 2022); (10) an organic soil layer representation at forest floors (Chen et al.,  
272 2016) and a microbial-explicit soil organic carbon decomposition model (MESDM; X. Zhang et  
273 al., 2022b); (11) coupling with atmospheric dry deposition of air pollutant (Chang et al., 2022);  
274 (12) enhanced permafrost soil representations (X. Li et al., 2020); (13) spring wheat crop dynamics  
275 (Zhang et al., 2023); (14) new treatment of thermal roughness length (Chen and Zhang 2009); (15)  
276 the Gecros crop model (Ingwersen et al., 2018; Warrach-Sagi et al., 2022); (16) a 1-D dual-  
277 permeability flow model (based on the mixed-form Richards' equation) representing preferential  
278 flow through variably-saturated soil with surface ponding being developed in the University of  
279 Arizona.

280

## 281 **2.6 Noah-MP multi-physics options**

282  
 283  
 284  
 285  
 286  
 287  
 288  
 289  
 290  
 291  
 292

One unique feature and advantage of Noah-MP is the inclusion of multiple physics options for different land processes for testing competing hypotheses (i.e., options) and multi-model ensemble simulations. Table 1 summarizes all the available physics options in the community Noah-MP v5.0. In particular, compared to previous Noah-MP versions, we have separated the runoff options for surface and subsurface runoff processes, and added a new physics option for snow thermal conductivity calculations, which were originally hard-coded without the namelist control capability. More detailed descriptions of each physics option are provided in the technical documentation (He et al., 2023).

**Table 1.** List of Noah-MP version 5.0 multi-physics options

<b>Noah-MP Physics</b>	<b>Option</b>	<b>Notes (* indicates the default option)</b>
OptDynamicVeg options for dynamic (prognostic) vegetation	1	off (use table LeafAreaIndex; use VegFrac = VegFracGreen from input) (Niu et al., 2011; Yang et al., 2011)
	2	on (together with OptStomataResistance = 1) (Dickinson et al., 1998; Niu and Yang, 2003)
	3	off (use table LeafAreaIndex; calculate VegFrac)
	4*	off (use table LeafAreaIndex; use maximum vegetation fraction)
	5	on (use maximum vegetation fraction)
	6	on (use VegFrac = VegFracGreen from input)
	7	off (use input LeafAreaIndex; use VegFrac = VegFracGreen from input)
	8	off (use input LeafAreaIndex; calculate VegFrac)
	9	off (use input LeafAreaIndex; use maximum vegetation fraction)
OptRainSnowPartition options for partitioning precipitation into rainfall & snowfall	1*	Jordan (1991) scheme
	2	BATS: when TemperatureAirRefHeight < freezing point+2.2 (Yang and Dickinson, 1996)
	3	TemperatureAirRefHeight < freezing point (Niu et al., 2011)
	4	Use WRF microphysics output (Barlage et al., 2015)
	5	Use wet-bulb temperature (Wang et al., 2019)
OptSoilWaterTranspiration options for soil moisture factor for stomatal resistance & ET	1*	Noah (soil moisture) (Ek et al., 2003)
	2	CLM (matric potential) (Oleson et al., 2004)
	3	SSiB (matric potential) (Xue et al., 1991)
OptGroundResistanceEvap options for ground resistant to evaporation/sublimation	1*	Sakaguchi and Zeng (2009) scheme
	2	Sellers (1992) scheme
	3	adjusted Sellers (1992) for wet soil
	4	Sakaguchi and Zeng (2009) for non-snow; rsurf = rsurf_snow for snow (set in NoahmpTable.TBL)
OptSurfaceDrag options for surface layer drag/exchange coefficient	1*	Monin-Obukhov (M-O) Similarity Theory (Brutsaert, 1982)
	2	original Noah (Chen et al. 1997)

OptStomataResistance	1*	Ball-Berry scheme (Ball et al., 1987; Bonan, 1996)
options for canopy stomatal resistance	2	Jarvis scheme (Jarvis, 1976)
OptSnowAlbedo	1*	BATS snow albedo (Dickinson et al., 1993)
options for ground snow surface albedo	2	CLASS snow albedo (Verseghy, 1991)
OptCanopyRadiationTransfer	1	modified two-stream (gap = $f(\text{solar angle}, 3\text{D structure, etc}) < 1 - \text{VegFrac}$ ) (Niu and Yang, 2004)
options for canopy radiation transfer	2	two-stream applied to grid-cell (gap=0) (Niu et al., 2011)
	3*	two-stream applied to vegetated fraction (gap=1-VegFrac) (Dickinson, 1983; Sellers, 1985)
OptSnowSoilTempTime	1*	semi-implicit; flux top boundary condition (Niu et al., 2011)
options for snow/soil temperature time scheme (only layer 1)	2	full implicit (original Noah); temperature top boundary condition (Ek et al., 2003)
	3	same as 1, but snow cover for skin temperature calculation (Niu et al., 2011)
OptSnowThermConduct	1*	Stieglitz scheme (Yen, 1965)
options for snow thermal conductivity	2	Anderson (1976) scheme
	3	Constant (Niu et al., 2011)
	4	Verseghy (1991) scheme
	5	Douvill scheme (Yen, 1981)
OptSoilTemperatureBottom	1	zero heat flux from bottom (DepthSoilTempBottom & TemperatureSoilBottom not used) (Niu et al., 2011)
options for lower boundary condition of soil temperature	2*	TemperatureSoilBottom at DepthSoilTempBottom (8m) read from a file (original Noah) (Ek et al., 2003)
OptSoilSupercoolWater	1*	No iteration (Niu and Yang, 2006)
options for soil supercooled liquid water	2	Koren's iteration (Koren et al., 1999)
OptRunoffSurface	1	TOPMODEL with groundwater (Niu et al., 2007)
options for surface runoff	2	TOPMODEL with an equilibrium water table (Niu et al., 2005)
	3*	Schaake scheme (original Noah) (Schaake et al., 1996)
	4	BATS surface and subsurface runoff (Yang and Dickinson, 1996)
	5	Miguez-Macho & Fan (MMF) groundwater scheme (Fan et al., 2007; Miguez-Macho et al. 2007)
	6	Variable Infiltration Capacity Model surface runoff scheme (Liang et al., 1994)
	7	Xinjiang Infiltration and surface runoff scheme (Jayawardena and Zhou, 2000)
	8	Dynamic VIC surface runoff scheme (Liang and Xie, 2003)

OptRunoffSubsurface options for drainage & subsurface runoff	1~8	similar to runoff option, separated from original Noah-MP runoff option, currently tested & recommended the same option# as surface runoff (default)
OptSoilPermeabilityFrozen options for frozen soil permeability	1*	linear effects, more permeable (Niu and Yang, 2006)
	2	nonlinear effects, less permeable (Koren et al., 1999)
OptDynVicInfiltration options for infiltration in dynamic VIC runoff scheme	1*	Philip scheme (Liang and Xie, 2003)
	2	Green-Ampt scheme (Liang and Xie, 2003)
	3	Smith-Parlange scheme (Liang and Xie, 2003)
OptTileDrainage options for tile drainage currently only tested & calibrated to work with runoff option=3	0*	No tile drainage
	1	on (simple scheme) (Valayamkunnath et al., 2022)
	2	on (Hooghoudt's scheme) (Valayamkunnath et al., 2022)
OptIrrigation options for irrigation	0*	No irrigation
	1	Irrigation on (Valayamkunnath et al., 2021)
	2	irrigation trigger based on crop season planting and harvesting dates (Valayamkunnath et al., 2021)
	3	irrigation trigger based on LeafAreaIndex threshold (Valayamkunnath et al., 2021)
OptIrrigationMethod options for irrigation method, only works when OptIrrigation > 0	0*	method based on geo_em fractions
	1	sprinkler method (Valayamkunnath et al., 2021)
	2	micro/drip irrigation (Valayamkunnath et al., 2021)
	3	surface flooding (Valayamkunnath et al., 2021)
OptCropModel options for crop model	0*	No crop model
	1	Liu, et al. (2016) crop scheme
OptSoilProperty options for defining soil properties	1*	use input dominant soil texture
	2	use input soil texture that varies with depth
	3	use soil composition (sand, clay, orgm) and pedotransfer function
	4	use input soil properties
OptPedotransfer options for pedotransfer functions, only works when OptSoilProperty=3	1*	Saxton and Rawls (2006) scheme
OptGlacierTreatment options for glacier treatment	1*	include phase change of glacier ice
	2	Glacier ice treatment more like original Noah

293

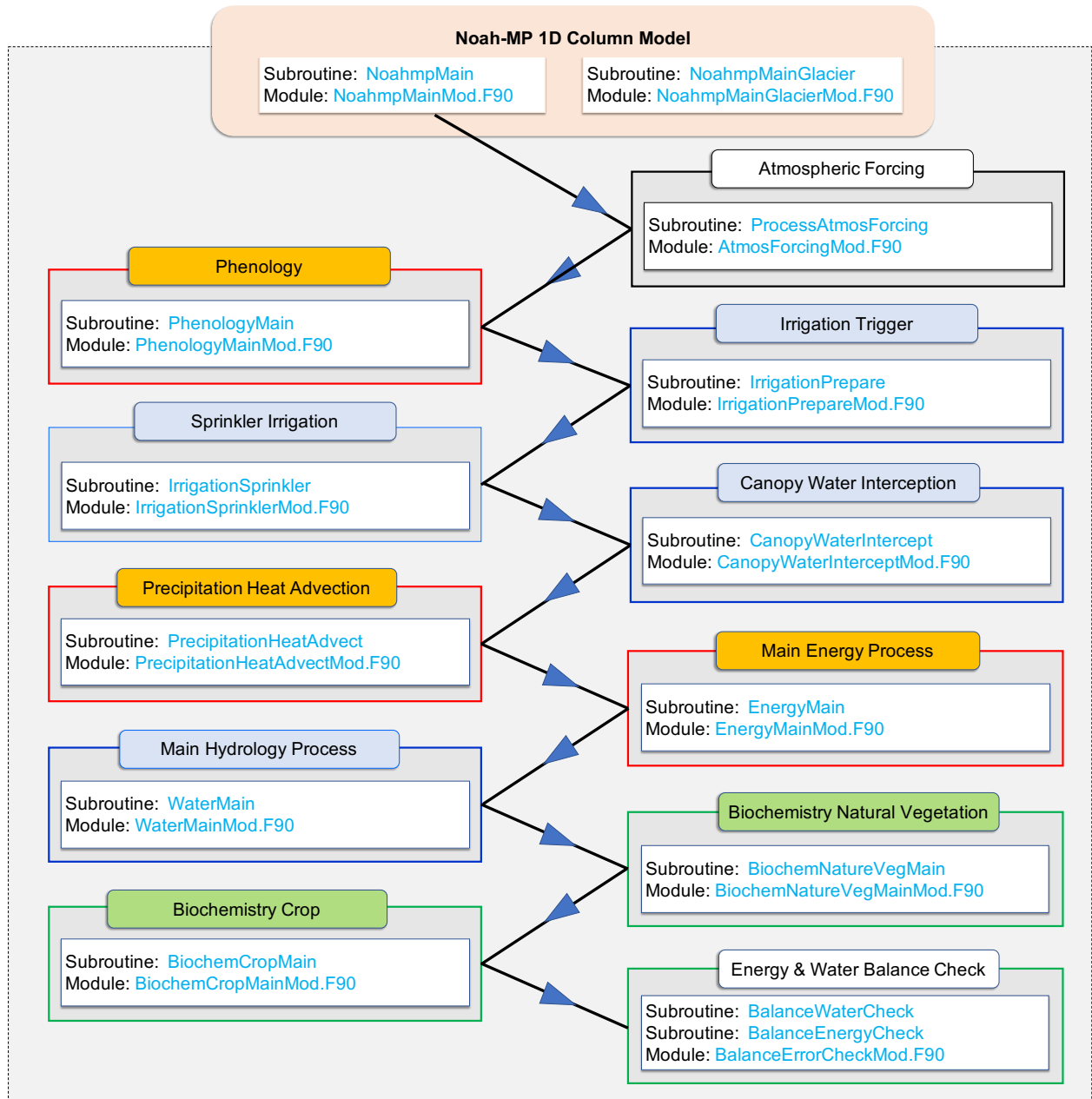
294

### 295 3. Enhanced model modularization in Noah-MP version 5.0

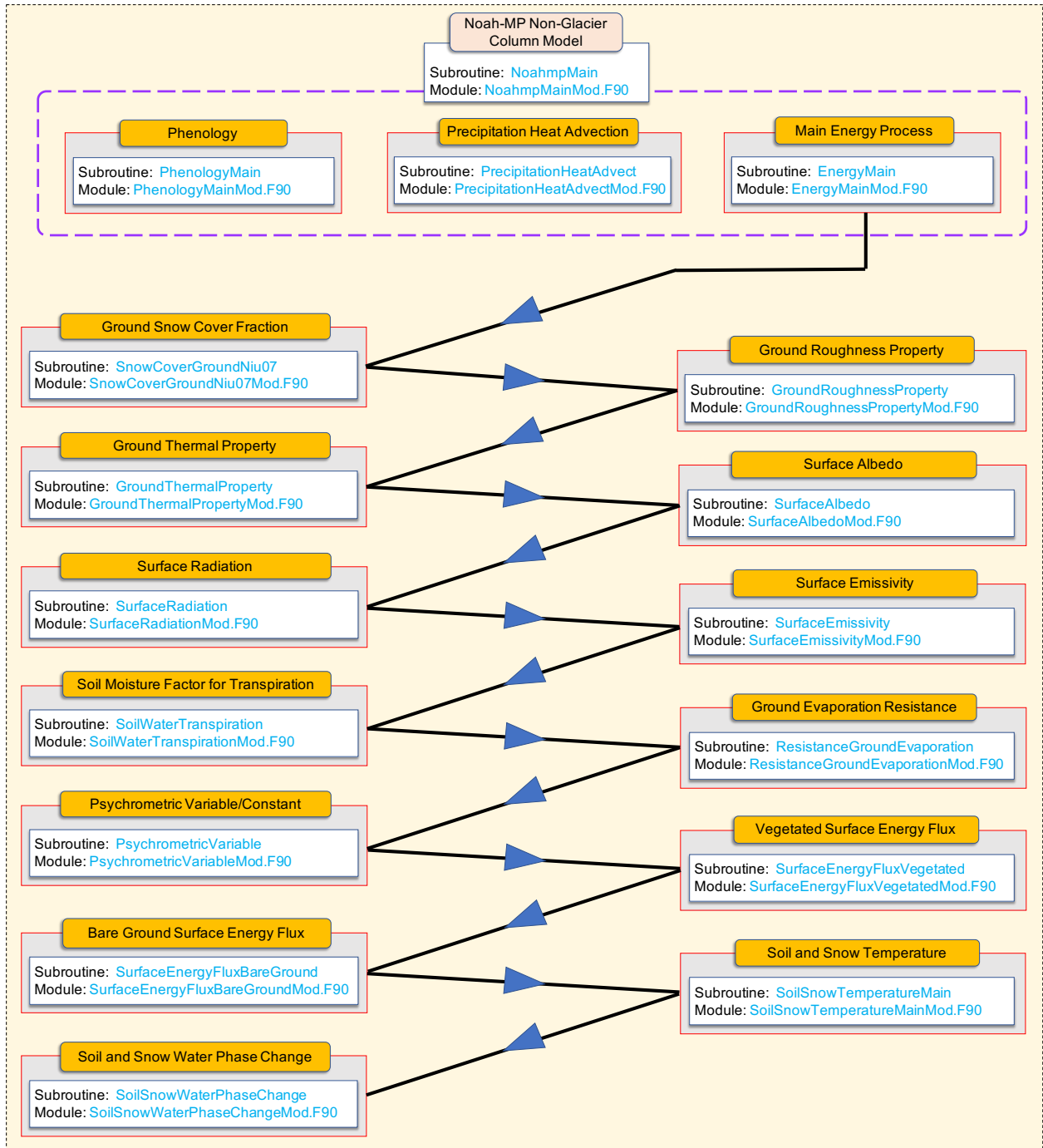
296

297 In the Noah-MP v5.0, we have modularized all model physics by separating and re-organizing  
298 each code subroutine into individual process-level Fortran module file with new descriptive, self-

299 explanatory module and subroutine names. As such, each model physics or scheme has its own  
300 separate module. Figure 4 shows the calling tree of the modularized Noah-MP main model physics  
301 workflow. Figures 5-7 show the calling tree of the modularized energy, water, and carbon  
302 processes, respectively. Compared to the previous Noah-MP versions that have a single lengthy  
303 source file lumping together all model subroutines with non-self-explanatory names, the highly-  
304 modularized model structure of the Noah-MP v5.0 provides a much more clear, neat, and  
305 organized way for users and developers to understand and follow the model logics and physics.  
306 These new modules use consistent coding format and standards, offering convenience for code  
307 reading, writing, and debugging. The highly-modularized model structure also allows external  
308 community weather/climate/hydrology models to easily adopt specific Noah-MP physical  
309 processes/schemes as independent process-level module files and implement them for testing and  
310 coupling.  
311

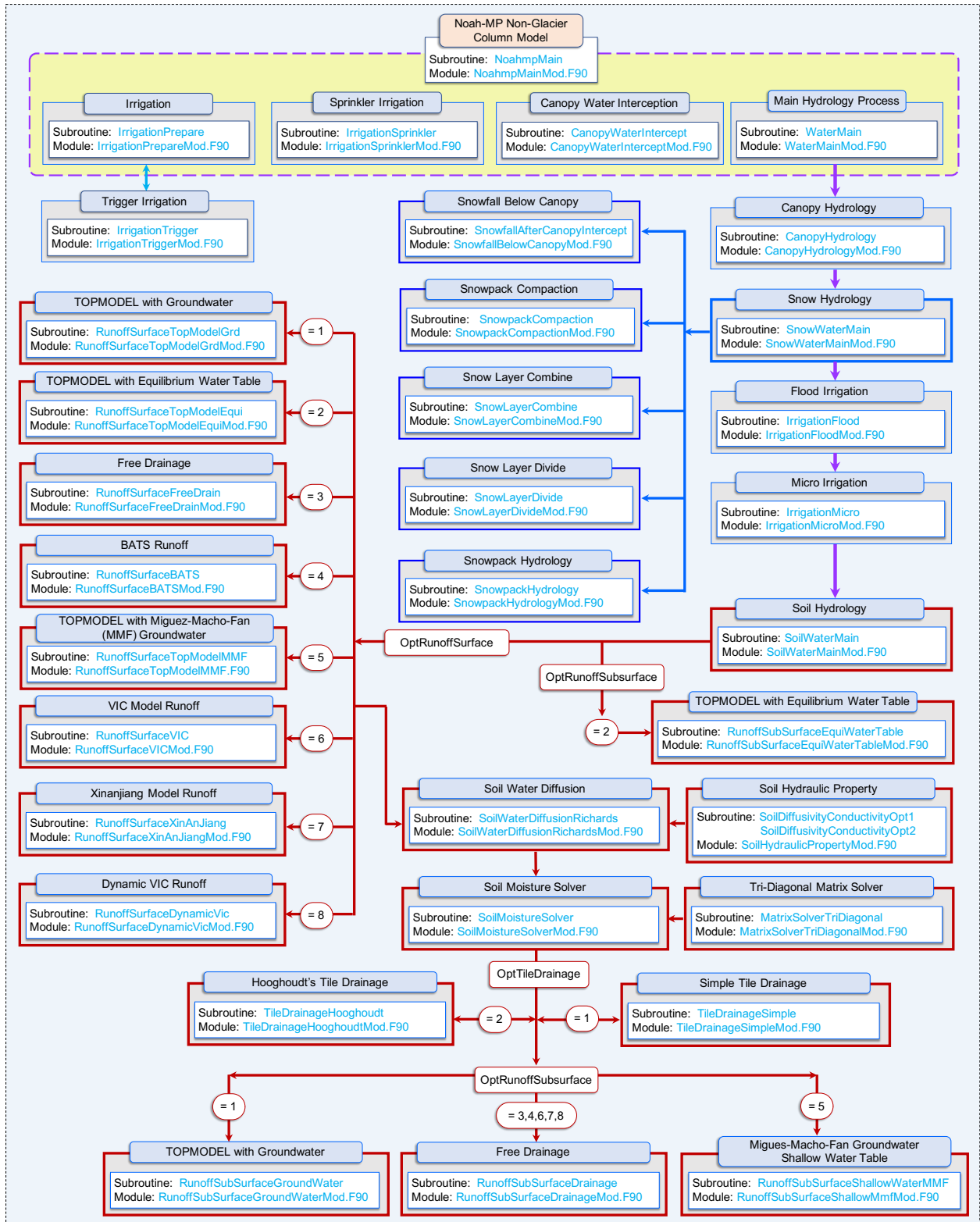


312  
 313 **Figure 4.** The modularized Noah-MP main physics calling tree in version 5.0. Blue boxes indicate  
 314 water processes, orange boxes indicate energy processes, and green boxes indicate biochemical  
 315 processes. The direction of arrows indicates processes calling sequence and information flow. Note  
 316 that the 1-D glacier column model has similar structures as the main non-glacier model, except  
 317 that the vegetation-related processes are removed and soil is replaced by glacier ice.  
 318

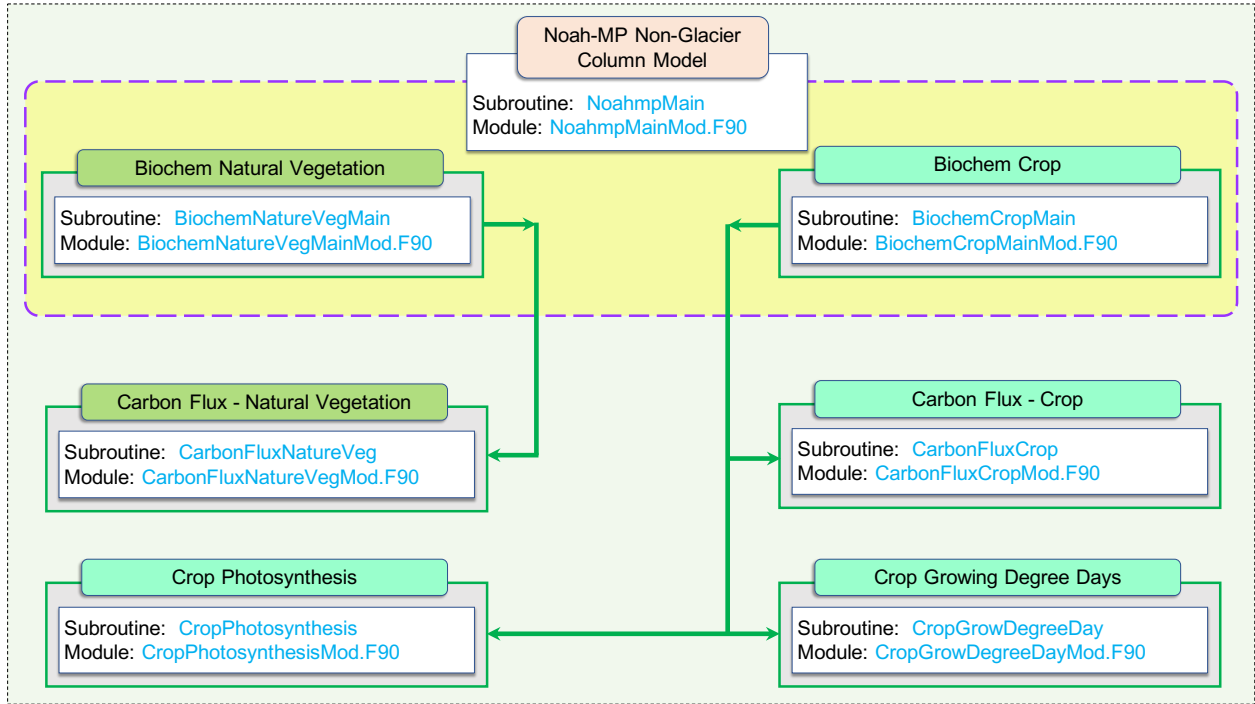


319  
 320 **Figure 5.** The modularized Noah-MP energy processes calling tree in version 5.0. Note that the  
 321 glacier model has similar structures except that the vegetation-related processes are removed and  
 322 soil is replaced by glacier ice.  
 323





324  
 325 **Figure 6.** The modularized Noah-MP water processes calling tree in version 5.0. Note that the  
 326 glacier model has similar structures except that it only includes the snowpack processes and soil  
 327 is replaced by glacier ice.



329

330 **Figure 7.** The modularized Noah-MP biochemical processes calling tree in version 5.0. Note that  
 331 currently the Noah-MP v5.0 only includes carbon processes. Note that the CropPhotosynthesis  
 332 module is not used currently to avoid inconsistency with the photosynthesis calculations from the  
 333 canopy stomatal resistance module.

334

335

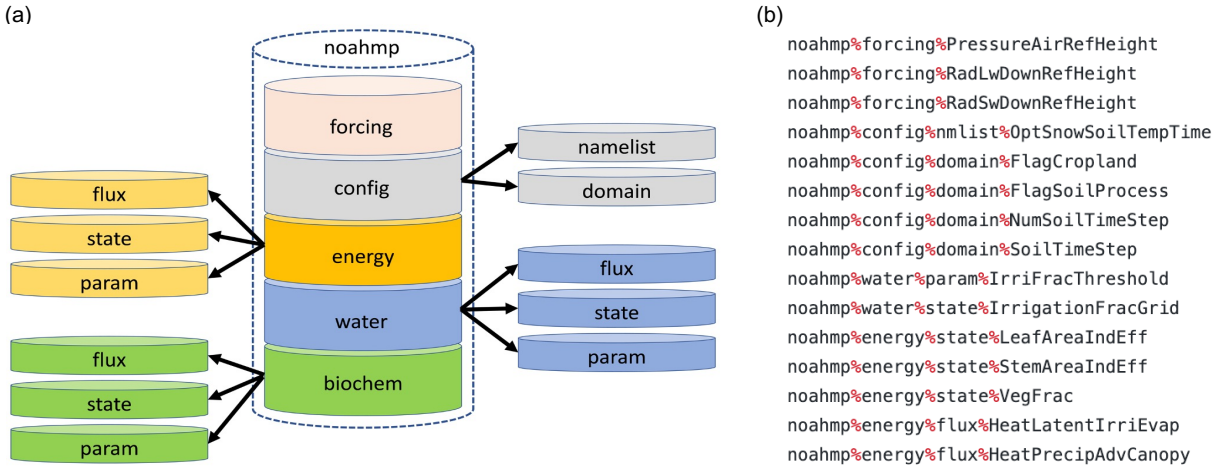
336 **4. Enhanced data structure in Noah-MP version 5.0**

337

338 In the Noah-MP v5.0, we have enhanced data structure with new hierarchical data types, which  
 339 allows a more efficient and convenient control of model variables and substantially simplifies code  
 340 structures and calling interface (Section 5). Figure 8 summarizes the new Noah-MP data type  
 341 hierarchy and gives some examples of model variable expression based on the hierarchical data  
 342 types. Specifically, we have defined an overarching “noahmp” main data type, which includes  
 343 “forcing” for atmospheric forcing variable type, “config” for model configuration variable type  
 344 with “domain” and “namelist” subtypes, “energy” for energy-related variable type, “water” for  
 345 water-related variable type, and “biochem” for biochemistry-related variable type. The “energy”,  
 346 “water”, and “biochem” types are further divided into “flux”, “state”, and “param” subtypes for  
 347 flux, state, and parameter variables. This hierarchical data structure provides a better organization  
 348 and management of model variables and their physical attributes. We have also optimized the  
 349 variable declaration and initialization structures based on those new data types and consistent  
 350 coding format and standard. In addition, we have re-defined many key local model state, flux, and  
 351 parameter variables in the base code to be global variables in the refactored code, which allows a

352 better track and management of these variables for diagnosis, transfer between Noah-MP and host  
 353 models, and coupling with data assimilation systems.

354  
 355



356  
 357 **Figure 8.** (a) The new hierarchical “noahmp” data types in the Noah-MP version 5.0. (b) Examples  
 358 of model variable expression using the hierarchical data types.

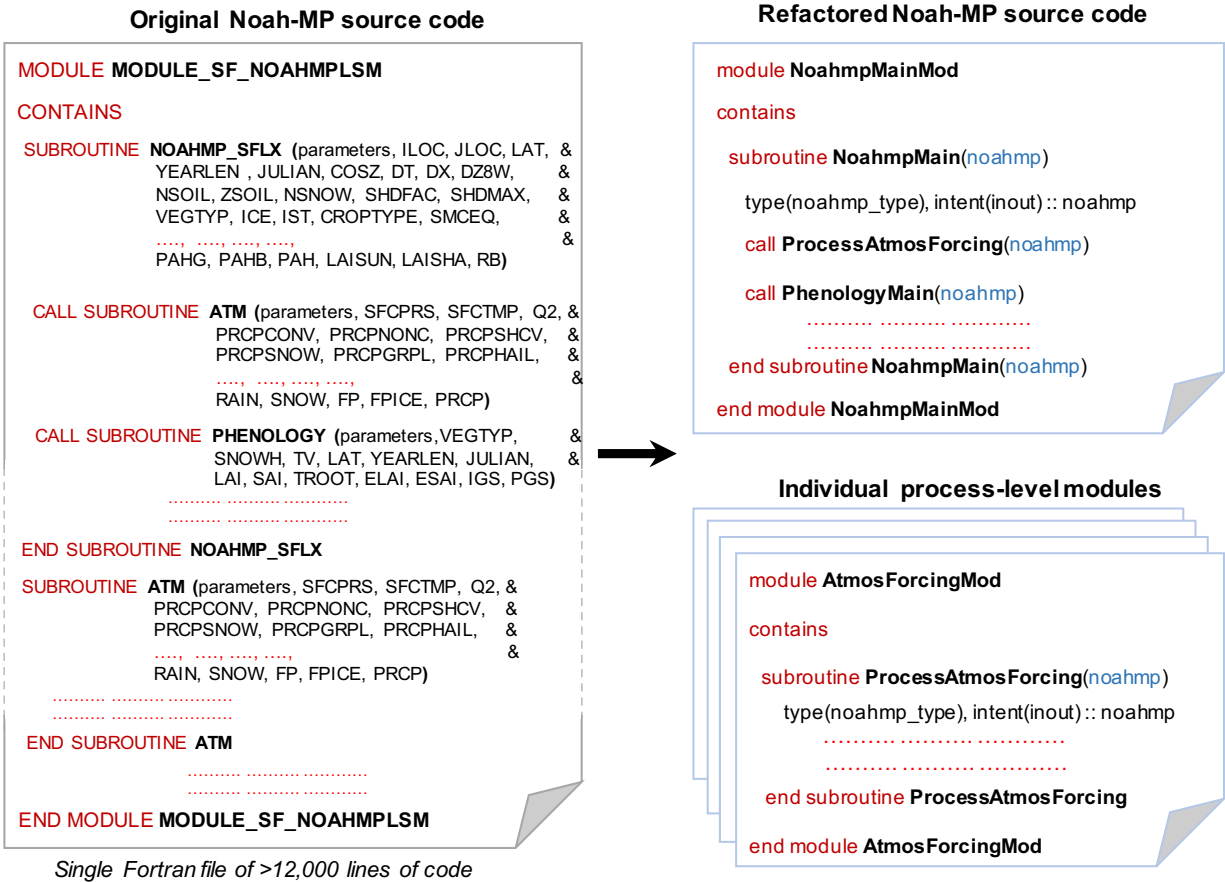
359  
 360

### 361 5. Enhanced code structure in Noah-MP version 5.0

362

363 Leveraging the model modularization (Section 3) and new data types (Section 4) in the Noah-MP  
 364 v5.0, we have further refined the code structure and subroutine interface. A graphical  
 365 representation of the refactored Noah-MP subroutine interface is depicted in Figure 9. Specifically,  
 366 the refined subroutine interface only requires passing the “noahmp” data type instead of each  
 367 individual variable names, because all relevant variables are defined and included in the “noahmp”  
 368 data type. This significantly simplifies the code structure with much more concise and neat  
 369 subroutine calls. The refined subroutine interface also makes future model development and code  
 370 changes simpler, more efficient, and less error-prone. For instance, if users want to add/remove a  
 371 variable for a specific physical scheme, they only need to edit as few as 3 module files: variable  
 372 type definition module, variable initialization module, the target physical scheme module, and if  
 373 needed, the variable input/output module. There is no need to go through and change all the  
 374 subroutine calls and interfaces that use the target variable.

375



376  
377 **Figure 9.** Demonstration of refactored subroutine interface and code structure in the Noah-MP  
378 version 5.0.

379  
380  
381 **6. Enhanced variable naming in Noah-MP version 5.0**

382  
383 In the Noah-MP v5.0, we have also renamed all the model variables using a more descriptive and  
384 self-explanatory naming standard, which clarifies the physical meaning of variables directly by  
385 their names and hence substantially lowers the hurdles of reading and understanding the code and  
386 model physics. The original variable names in the previous Noah-MP versions are hard to  
387 understand, in which case users have to check back and forth the variable definition to know their  
388 physical meaning. For instance, the original variable name for canopy intercepted total water is  
389 “CMC”, while the new name is “CanopyTotalWater”. Table 2 gives more examples of the  
390 enhanced variable naming in Noah-MP v5.0. A detailed Noah-MP variable glossary listing  
391 variables’ original and new names, physical meaning, data type, and unit is provided in the  
392 technical documentation (He et al., 2023) and the community Noah-MP GitHub repository.

396 **Table 2.** Examples of new variable names based on a more descriptive and self-explanatory  
 397 naming standard in the Noah-MP version 5.0, compared with the original names.

Variable physical meaning/definition	New name	Original name	Variable Type	Unit
wetted or snowed fraction of canopy	CanopyWetFrac	FWET	Real	-
canopy intercepted liquid water	CanopyLiqWater	CANLIQ	Real	mm
canopy intercepted ice	CanopyIce	CANICE	Real	mm
canopy intercepted total water	CanopyTotalWater	CMC	Real	mm
canopy capacity for snow interception	CanopyIceMax	MAXSNO	Real	mm
canopy capacity for liquid water interception	CanopyLiqWaterMax	MAXLIQ	Real	mm
ice fraction in snow layers	SnowIceFrac	FICE_SNOW	Real	-
bulk density of snowfall	SnowfallDensity	BDFALL	Real	kg/m <sup>3</sup>
snow cover fraction	SnowCoverFrac	FSNO	Real	-
snow layer ice	SnowIce	SNICE	Real	mm
snow layer liquid water	SnowLiqWater	SNLIQ	Real	mm

398

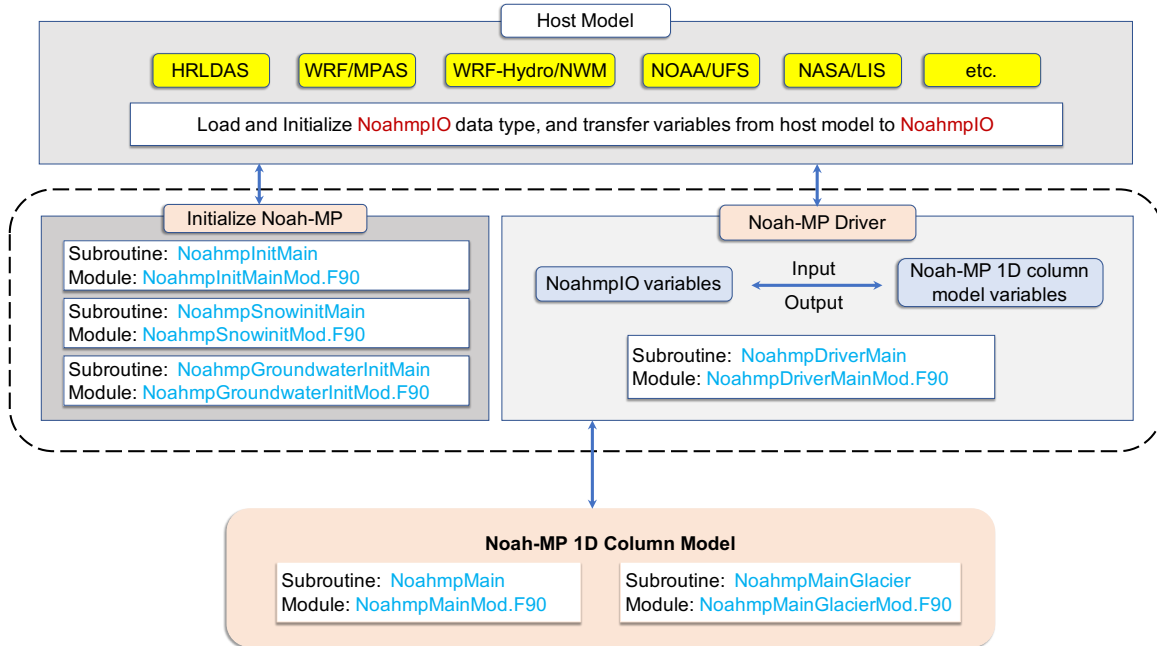
399

400 **7. Enhanced coupling structure with host models in Noah-MP version 5.0**

401

402 We have further updated the Noah-MP driver and interface coupled with potential host  
 403 weather/climate/hydrology models. Figure 10 summarizes the interface and coupling structures in  
 404 the Noah-MP v5.0. Specifically, the coupling interface includes: (1) defining a 2-D (for structured  
 405 grid mesh) or vectorized (for unstructured grid mesh) Noah-MP input/output data type  
 406 “NoahmpIO” to facilitate the input/output communication between host models and the core  
 407 Noah-MP 1-D column model (“noahmp” data type); (2) the initialization of the “NoahmpIO”  
 408 variables with values from host models; (3) the main Noah-MP driver that calls the core 1-D  
 409 column model and transfers between the “NoahmpIO” and “noahmp” variables as part of  
 410 input/output processes. Currently, the coupling of the Noah-MP v5.0 with the NCAR/HRLDAS  
 411 system has been successfully completed. The coupling of Noah-MP v5.0 with the NASA/LIS  
 412 system and the WRF-Hydro/NWM system is on-going. We also plan to couple the Noah-MP v5.0  
 413 with other host models in the future (Section 9), such as WRF, MPAS, and NOAA/UFS. Because  
 414 of the enhanced coupling interface and structure in Noah-MP v5.0, we will only need to slightly  
 415 adapt the coupling interface and driver to allow it to work with different host models. We will  
 416 manage and maintain the interface and driver code for each host model in the community Noah-  
 417 MP GitHub repository to ensure the compatibility between host models and updated core Noah-  
 418 MP source code in the future, which will allow smooth transition and seamless synthesizing of  
 419 Noah-MP updates in host models.

420



421  
 422 **Figure 10.** Workflow of the Noah-MP v5.0 driver and interface structures to couple with various  
 423 host weather/climate/hydrology models.  
 424

425  
 426 **8. Benchmarking for Noah-MP version 5.0**  
 427

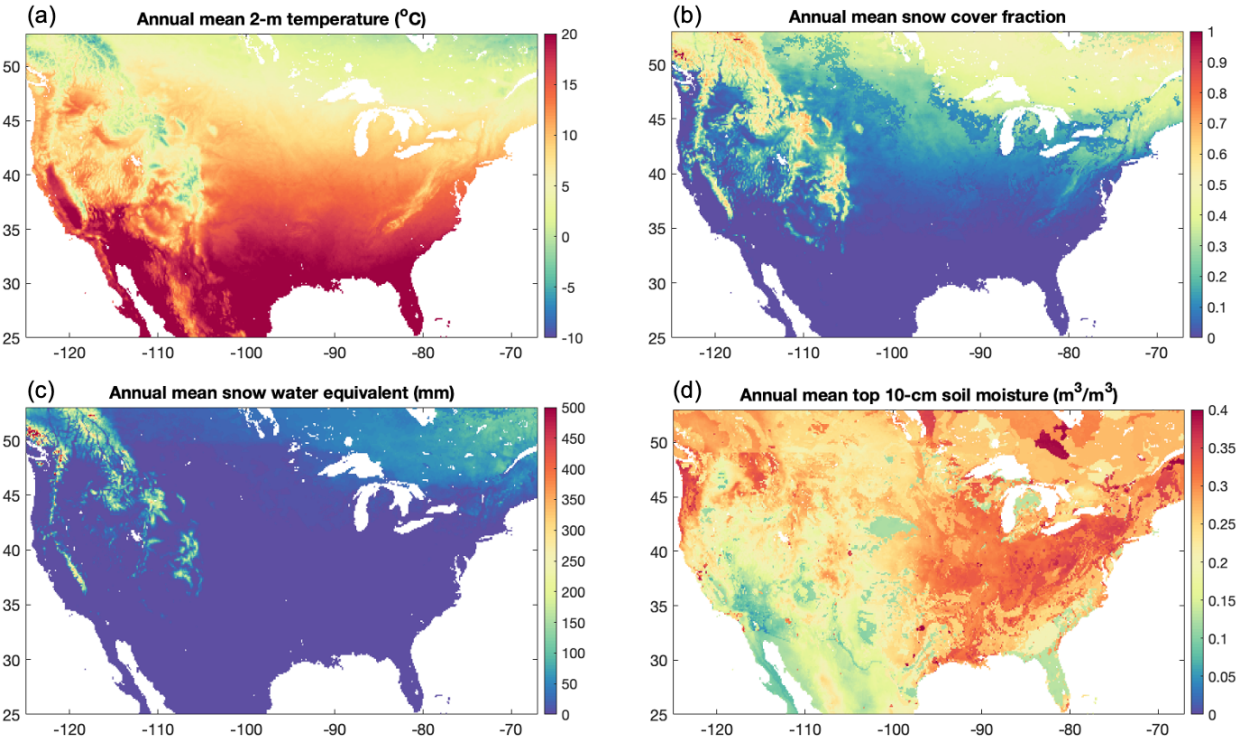
428 To benchmark the functionality, reproducibility, and computational efficiency of the modernized  
 429 Noah-MP code, we have conducted a series of hierarchical test simulations during the course of  
 430 Noah-MP refactoring. Specifically, after refactoring each major Noah-MP model  
 431 component/physics (e.g., water, energy, carbon, etc.) listed in Figure 4, we built simple driver  
 432 modules to conduct benchmark simulations using each of these model component/physics to test  
 433 and ensure the bit-for-bit consistency between the refactored code and base code for all Noah-MP  
 434 physics options. Here is an example for the refactored Noah-MP water component model we built  
 435 for benchmarking during the course of refactoring:  
 436 [https://github.com/cenlinhe/NoahMP\\_refactor/tree/water\\_refactor](https://github.com/cenlinhe/NoahMP_refactor/tree/water_refactor), which was used to test the bit-  
 437 for-bit consistency between the refactored and base Noah-MP water component codes.  
 438

439 After we completed the entire model refactoring, we have conducted another set of test simulations  
 440 using the completed Noah-MP v5.0 to ensure its bit-for-bit consistency with the base model code  
 441 for all different combinations of physics options as well as to benchmark its computational  
 442 efficiency. These tests were conducted via 1-year point-scale SNOTEL 804-site simulations, 1-  
 443 year 12-km gridded continental US simulations, and 1-year 1-km gridded simulations over central  
 444 US agricultural regions (particularly to test individual and combination of physics options related  
 445 to crop, irrigation, tile drainage, and groundwater). The tests all showed exactly the same results  
 446 between the refactored and base simulations, with similar computational efficiency.



447  
448  
449  
450  
451  
452  
453  
454  
455  
456  
457  
458  
459  
460

In addition, in order to provide the community with reference Noah-MP v5.0 model datasets for future comparison and assessment, we have conducted 3 sets of benchmark simulations, including 21-year (2000-2020) 12-km continental US simulations driven by the NLDAS-2 atmospheric forcings (Xia et al., 2012), 10-year (2009-2018) point-scale SNOTEL 804-site simulations over the western US driven by observed precipitation and temperature as well as other NLDAS-2 atmospheric forcings downscaled to 90-m spatial resolution (He et al., 2021), and 1-year (2000) 4-km dynamic crop simulations over the U.S. Corn Belt region driven by the convection-permitting WRF modeling (Zhang et al., 2020). We have archived all the atmospheric forcing datasets, model setup input datasets, and model output datasets for these benchmark simulations. Figure 11 shows an example of the model output. Note that a comprehensive evaluation of the simulation results is outside the scope of this model description paper and will be done in the next step.



461  
462 **Figure 11.** Demonstration of 20-year (2001-2020) annual mean (a) 2-m temperature, (b) snow  
463 cover fraction, (c) snow water equivalent, and (d) top 10-cm soil moisture from the Noah-MP  
464 version 5.0 12-km continental US benchmark simulations driven by the NLDAS-2 atmospheric  
465 forcings.

466  
467  
468

### 9. Model code and technical documentation for Noah-MP version 5.0

469 We archive, manage, and maintain the Noah-MP v5.0 (together with previous code versions) at  
470 the NCAR community Noah-MP GitHub repository (<https://github.com/NCAR/noahmp>) for



471 public access. We have also created a comprehensive technical documentation (He et al., 2023)  
472 for the Noah-MP v5.0, available at <http://dx.doi.org/10.5065/ew8g-yr95>, which provides detailed  
473 descriptions of model physics and formulations.

474

## 475 **10. Conclusions and future plans**

476

477 In this study, we modernized the widely-used state-of-the-art Noah-MP LSM by adopting modern  
478 Fortran code and data structures and standards, which substantially enhances the model modularity,  
479 interoperability, and applicability. The modernized Noah-MP has been released as the model  
480 version 5.0, which includes the following key features: (1) enhanced modularization and  
481 interoperability by re-organizing model physics into individual process-level Fortran module files,  
482 (2) enhanced data structure with new hierarchical data types and optimized variable declaration  
483 and initialization structures, (3) enhanced code structure and calling workflow by leveraging the  
484 new data structure and modularization, (4) enhanced (descriptive and self-explanatory) model  
485 variable naming standard, and (5) enhanced driver and interface structure to couple with host  
486 weather/climate/hydrology models. The base code used for modernization is the Noah-MP version  
487 4.5 (released in December 2022), and the modernization effort does not change model physics. In  
488 addition, we have created a comprehensive technical documentation (He et al., 2023) of the Noah-  
489 MP v5.0, and a set of benchmark simulation datasets. The Noah-MP v5.0 has been coupled to the  
490 NCAR/HRLDAS system. Currently, the work of coupling the Noah-MP v5.0 with the latest  
491 NASA/LIS system and the WRF-Hydro/NWM system is on-going. In the future, we also plan to  
492 couple the Noah-MP v5.0 to other weather and climate models, including WRF, MPAS, and  
493 NOAA/UFS. Overall, the modernized open-source community Noah-MP model will allow a more  
494 efficient and convenient process for future model developments and applications.

495

496

### 497 **Code and data availability**

498 1. The Noah-MP model code (<https://doi.org/10.5281/zenodo.7901855>) is available at  
499 <https://github.com/NCAR/noahmp>

500 2. The coupled HRLDAS/Noah-MP model code (<https://doi.org/10.5281/zenodo.7901867>) is  
501 available at <https://github.com/NCAR/hrldas>

502 3. The Noah-MP technical documentation is available at <http://dx.doi.org/10.5065/ew8g-yr95>

503 4. The benchmark datasets [are stored in the NCAR high-performance supercomputer \(HPC\)](#)  
504 [campaign storage file system \(data path: /glade/campaign/ral/hap/cenlinhe/NoahMP\\_benchmark/](#)  
505 [see details about the storage system at https://arc.ucar.edu/knowledge\\_base/70549621\)](#) and can be  
506 provided by the corresponding author upon request, due to the extremely large data size (8.8 TB).

507

508

### 509 **Author contribution**

510 CH, PV, and MB led the code refactoring effort with the help from all the other coauthors (FC,  
511 DG, RC, GN, ZY, DN, ME, TS, RR). CH and PV led the technical documentation writing effort  
512 with the help from all the other coauthors (MB, FC, DG, RC, GN, ZY, DN, ME, TS, RR). CH  
513 conducted the benchmark model simulations. CH drafted the manuscript with improvements from  
514 all the other coauthors (PV, FC, MB, DG, RC, GN, ZY, DN, ME, TS, RR).

515

516

### 517 **Competing interests**

518 The authors declare that they have no conflict of interest.

519

520

### 521 **Acknowledgements**

522 We thank Zhe Zhang (NCAR) and Ronnie Abolafia-Rosenzweig (NCAR) for helping with model  
523 code testing and for helpful discussions. We also acknowledge the strong support from the entire  
524 Noah-MP community. This study was supported by the US Geological Survey (USGS) Water  
525 Mission Area's Integrated Water Prediction Program, NOAA's Climate Program Office's  
526 Modeling, Analysis, Predictions, and Projections Program (MAPP), and the NCAR Water System  
527 Program. National Center for Atmospheric Research (NCAR) is a major facility sponsored by the  
528 National Science Foundation (NSF) under Cooperative Agreement #1852977. Any opinions,  
529 findings, conclusions, or recommendations expressed in this publication are those of the authors  
530 and do not necessarily reflect the views of the National Science Foundation.

531

532

### 533 **References**

- 534 Abolafia-Rosenzweig, R., He, C., Burns, S.P., Chen, F., 2021. Implementation and Evaluation of  
535 a Unified Turbulence Parameterization Throughout the Canopy and Roughness Sublayer in  
536 Noah-MP Snow Simulations. *J Adv Model Earth Syst* 13.  
537 <https://doi.org/10.1029/2021MS002665>
- 538 Abolafia-Rosenzweig, R., He, C., Chen, F., 2022a. Winter and spring climate explains a large  
539 portion of interannual variability and trend in western U.S. summer fire burned area. *Environ.*  
540 *Res. Lett.* 17, 054030. <https://doi.org/10.1088/1748-9326/ac6886>
- 541 Abolafia-Rosenzweig, R., He, C., McKenzie Skiles, S., Chen, F., Gochis, D., 2022b. Evaluation  
542 and Optimization of Snow Albedo Scheme in Noah-MP Land Surface Model Using In Situ  
543 Spectral Observations in the Colorado Rockies. *J Adv Model Earth Syst* 14.  
544 <https://doi.org/10.1029/2022MS003141>
- 545 Abolafia-Rosenzweig, R., He, C., Chen, F. et al. 2023a. High Resolution Forecasting of Summer  
546 Drought in the Western United States. *Water Resources Research*, in review
- 547 Abolafia-Rosenzweig, R., He, C., Chen, F. et al. 2023b. Evaluating Noah-MP simulated post-fire  
548 runoff and snowpack in Pacific-Northwest: challenges and future improvements, *Water*  
549 *Resources Research*, in review

550 Anderson, E. A. (1976), A point energy and mass balance model of a snow cover, NOAA Tech.  
551 Rep. NWS 19, 150 pp., Off. of Hydrol., Natl. Weather Serv., Silver Spring, Md.

552 Arsenault, K. R., Shukla, S., Hazra, A., Getirana, A., McNally, A., Kumar, S. V., ... & Verdin, J.  
553 P. (2020). Better Advance Warnings of Drought. *Bulletin of the American Meteorological*  
554 *Society*, 101(10), 899-903.

555 Ball, J. T., I. E. Woodrow, and J. A. Berry (1987), A model predicting sto- matal conductance and  
556 its contribution to the control of photosynthesis under different environmental conditions, in  
557 *Process in Photosynthesis Research*, vol. 1, edited by J. Biggins, pp. 221–234, Martinus Nijhoff,  
558 Dordrecht, Netherlands.

559 Barlage, M., Tewari, M., Chen, F., Miguez-Macho, G., Yang, Z. L., & Niu, G. Y. (2015). The  
560 effect of groundwater interaction in North American regional climate simulations with  
561 WRF/Noah-MP. *Climatic Change*, 129, 485-498.

562 Barlage, M., Chen, F., Rasmussen, R., Zhang, Z., & Miguez-Macho, G. (2021). The importance  
563 of scale-dependent groundwater processes in land-atmosphere interactions over the central  
564 United States. *Geophysical Research Letters*, 48(5), e2020GL092171.

565 Blyth, E. M., Arora, V. K., Clark, D. B., Dadson, S. J., De Kauwe, M. G., Lawrence, D. M., ... &  
566 Yuan, H. (2021). Advances in land surface modelling. *Current Climate Change Reports*, 7(2),  
567 45-71.

568 Bonan, G. B. (1996), A land surface model (LSM version 1.0) for ecolog- ical, hydrological, and  
569 atmospheric studies: Technical description and user’s guide, NCAR Tech. Note NCAR/TN-  
570 417+STR, 150 pp., Natl. Cent. for Atmos. Res., Boulder, Colo.

571 Bonan, G. B., & Doney, S. C. (2018). Climate, ecosystems, and planetary futures: The challenge  
572 to predict life in Earth system models. *Science*, 359(6375), eaam8328.  
573 <https://doi.org/10.1126/science.aam8328>

574 Brunsell, N. A., de Oliveira, G., Barlage, M., Shimabukuro, Y., Moraes, E., & Aragao, L. (2021).  
575 Examination of seasonal water and carbon dynamics in eastern Amazonia: a comparison of  
576 Noah-MP and MODIS. *Theoretical and Applied Climatology*, 143, 571-586.

577 Brutsaert, W. A. (1982), *Evaporation Into the Atmosphere*, 299 pp., D. Reidel, Dordrecht,  
578 Netherlands.

579 Cai, X., Yang, Z. L., David, C. H., Niu, G. Y., & Rodell, M. (2014). Hydrological evaluation of  
580 the Noah-MP land surface model for the Mississippi River Basin. *Journal of Geophysical*  
581 *Research: Atmospheres*, 119(1), 23-38.

582 Cai, X., Yang, Z. L., Fisher, J. B., Zhang, X., Barlage, M., & Chen, F. (2016). Integration of  
583 nitrogen dynamics into the Noah-MP land surface model v1. 1 for climate and environmental  
584 predictions. *Geoscientific Model Development*, 9(1), 1-15.

585 Chang, M., Cao, J., Zhang, Q., Chen, W., Wu, G., Wu, L., ... & Wang, X. (2022). Improvement of  
586 stomatal resistance and photosynthesis mechanism of Noah-MP-WDDM (v1. 42) in simulation  
587 of NO<sub>2</sub> dry deposition velocity in forests. *Geoscientific Model Development*, 15(2), 787-801.

588 Chen, F., & Dudhia, J. (2001). Coupling an advanced land surface–hydrology model with the Penn  
589 State–NCAR MM5 Modeling System. Part I: Model implementation and sensitivity. *Monthly*  
590 *Weather Review*, 129, 17. [https://doi.org/10.1175/1520-0493\(2001\)129<0569:caalsh>2.0.co;2](https://doi.org/10.1175/1520-0493(2001)129<0569:caalsh>2.0.co;2)

591 Chen, F., Janjić, Z., & Mitchell, K. (1997). Impact of atmospheric surface-layer parameterizations  
592 in the new land-surface scheme of the NCEP Mesoscale Eta Model. *Boundary-Layer*  
593 *Meteorology*, 85, 391–421. <https://doi.org/10.1023/A:1000531001463>

594 Chen, F., Mitchell, K., Schaake, J., Xue, Y., Pan, H.-L., Koren, V., et al. (1996). Modeling of land  
595 surface evaporation by four schemes and comparison with FIFE observations. *Journal of*  
596 *Geophysical Research: Atmospheres*, 101, 7251–7268. <https://doi.org/10.1029/95JD02165>

597 Chen, F., & Zhang, Y. (2009). On the coupling strength between the land surface and the  
598 atmosphere: From viewpoint of surface exchange coefficients. *Geophysical Research*  
599 *Letters*, 36(10).

600 Chen, L., Li, Y., Chen, F., Barr, A., Barlage, M., & Wan, B. (2016). The incorporation of an  
601 organic soil layer in the Noah-MP land surface model and its evaluation over a boreal aspen  
602 forest. *Atmospheric Chemistry and Physics*, 16(13), 8375-8387.

603 Dickinson, R. E. (1983), Land surface processes and climate-surface albedo and energy balance,  
604 in *Theory of Climate*, Adv. Geophys., vol. 25, edited by B. Saltzman, pp. 305–353, Academic,  
605 San Diego, Calif.

606 Dickinson, R. E., A. Henderson-Sellers, and P. J. Kennedy (1993), Bio- sphere-Atmosphere  
607 Transfer Scheme (BATS) version 1e as coupled to the NCAR Community Climate Model,  
608 NCAR Tech. Note NCAR/TN- 387+STR, 80 pp., Natl. Cent. for Atmos. Res., Boulder, Colo.

609 Dickinson, R. E., M. Shaikh, R. Bryant, and L. Graumlich (1998), Interac- tive canopies for a  
610 climate model, *J. Clim.*, 11, 2823–2836, doi:10.1175/ 1520-  
611 0442(1998)011<2823:ICFACM>2.0.CO;2.

612 Ek, M. B., Mitchell, K. E., Lin, Y., Rogers, E., Grunmann, P., Koren, V., et al. (2003).  
613 Implementation of Noah land surface model advances in the National Centers for  
614 Environmental Prediction operational mesoscale Eta model. *Journal of Geophysical Research:*  
615 *Atmospheres*, 108, 2002JD003296. <https://doi.org/10.1029/2002JD003296>

616 Fan, Y., Miguez-Macho, G., Weaver, C. P., Walko, R., & Robock, A. (2007). Incorporating water  
617 table dynamics in climate modeling: 1. Water table observations and equilibrium water table  
618 simulations. *Journal of Geophysical Research: Atmospheres*, 112(D10).

619 Gao, Y., Xiao, L., Chen, D., Chen, F., Xu, J., & Xu, Y. (2017). Quantification of the relative role  
620 of land-surface processes and large-scale forcing in dynamic downscaling over the Tibetan  
621 Plateau. *Climate Dynamics*, 48, 1705-1721.

622 Hazra, A., McNally, A., Slinski, K., Arsenault, K. R., Shukla, S., Getirana, A., ... & Koster, R. D.  
623 (2023). NASA’s NMME-based S2S hydrologic forecast system for food insecurity early  
624 warning in southern Africa. *Journal of Hydrology*, 617, 129005.

625 He, C., F. Chen, M. Barlage, C. Liu, A. Newman, W. Tang, K. Ikeda, and R. Rasmussen (2019):  
626 Can convection-permitting modeling provide decent precipitation for offline high-resolution

627 snowpack simulations over mountains, J. Geophys. Res.-Atmos,  
628 124, <https://doi.org/10.1029/2019JD030823>

629 He, C., F. Chen, R. Abolafia-Rosenzweig, K. Ikeda, C. Liu, and R. Rasmussen (2021): What  
630 causes the unobserved early-spring snowpack ablation in convection-permitting WRF modeling  
631 over Utah mountains?, J. Geophys. Res.-Atmos, 126(22),  
632 e2021JD035284, <https://doi.org/10.1029/2021JD035284>

633 He, C., P. Valayamkunnath, M. Barlage, F. Chen, D. Gochis, R. Cabell, T. Schneider, R.  
634 Rasmussen, G.-Y. Niu, Z.-L. Yang, D. Niyogi, and M. Ek (2023): The Community Noah-MP  
635 Land Surface Modeling System Technical Description Version 5.0. (No. NCAR/TN-575+STR),  
636 <http://dx.doi.org/10.5065/ew8g-yr95>

637 Ingwersen, J., Högy, P., Wizemann, H. D., Warrach-Sagi, K., & Streck, T. (2018). Coupling the  
638 land surface model Noah-MP with the generic crop growth model Gecros: Model description,  
639 calibration and validation. *Agricultural and forest meteorology*, 262, 322-339.

640 Jarvis, P. G. (1976), The interpretation of the variations in leaf water poten- tial and stomatal  
641 conductance found in canopies in the field, *Philos. Trans. R. Soc. B*, 273, 593–610,  
642 doi:10.1098/rstb.1976.0035.

643 Jayawardena, A. W. and Zhou, M. C.: A modified spatial soil moisture storage capacity  
644 distribution curve for the Xinanjiang model, *Journal of Hydrology*, 227, 93–113,  
645 [https://doi.org/10.1016/S0022-1694\(99\)00173-0](https://doi.org/10.1016/S0022-1694(99)00173-0), 2000.

646 Jiang, Y., Chen, F., Gao, Y., He, C., Barlage, M., & Huang, W. (2020). Assessment of uncertainty  
647 sources in snow cover simulation in the Tibetan Plateau. *Journal of Geophysical Research:*  
648 *Atmospheres*, 125(18), e2020JD032674.

649 Jiang, Y., Gao, Y., He, C., Liu, B., Pan, Y., & Li, X. (2021). Spatiotemporal distribution and  
650 variation of wind erosion over the Tibetan Plateau based on a coupled land-surface wind-  
651 erosion model. *Aeolian Research*, 50, 100699.

652 Jordan, R. (1991), A one-dimensional temperature model for a snow cover, *Spec. Rep. 91–16*,  
653 *Cold Reg. Res. and Eng. Lab., U.S. Army Corps of Eng., Hanover, N. H.*

654 Ju, C., Li, H., Li, M., Liu, Z., Ma, Y., Mamtimin, A., ... & Song, Y. (2022). Comparison of the  
655 Forecast Performance of WRF Using Noah and Noah-MP Land Surface Schemes in Central  
656 Asia Arid Region. *Atmosphere*, 13(6), 927.

657 Koren, V., J. C. Schaake, K. E. Mitchell, Q.-Y. Duan, F. Chen, and J. M. Baker (1999), A  
658 parameterization of snowpack and frozen ground intended for NCEP weather and climate  
659 models, *J. Geophys. Res.*, 104, 19,569–19,585, doi:10.1029/1999JD900232.

660 Kumar, S. V., Holmes, T., Andela, N., Dharssi, I., Hain, C., Peters-Lidard, C., ... & Getirana, A.  
661 (2021). The 2019–2020 Australian drought and bushfires altered the partitioning of  
662 hydrological fluxes. *Geophysical Research Letters*, 48(1), e2020GL091411.

663 Li, X., Wu, T., Zhu, X., Jiang, Y., Hu, G., Hao, J., ... & Ying, X. (2020). Improving the Noah-MP  
664 model for simulating hydrothermal regime of the active layer in the permafrost regions of the  
665 Qinghai-Tibet Plateau. *Journal of Geophysical Research: Atmospheres*, 125(16),  
666 e2020JD032588.

667 Li, J., Chen, F., Lu, X., Gong, W., Zhang, G., & Gan, Y. (2020). Quantifying contributions of  
668 uncertainties in physical parameterization schemes and model parameters to overall errors in  
669 Noah-MP dynamic vegetation modeling. *Journal of Advances in Modeling Earth Systems*, 12.  
670 <https://doi.org/10.1029/2019MS001914>

671 Li, L., Yang, Z. L., Matheny, A. M., Zheng, H., Swenson, S. C., Lawrence, D. M., ... & Leung, L.  
672 R. (2021). Representation of plant hydraulics in the Noah-MP land surface model: Model  
673 development and multiscale evaluation. *Journal of Advances in Modeling Earth Systems*, 13(4),  
674 e2020MS002214.

675 Li, M., Wu, P., Ma, Z., Lv, M., Yang, Q., & Duan, Y. (2022). The decline in the groundwater table  
676 depth over the past four decades in China simulated by the Noah-MP land model. *Journal of*  
677 *Hydrology*, 607, 127551.

678 Liang, J., Yang, Z., & Lin, P. (2019). Systematic hydrological evaluation of the Noah-MP land  
679 surface model over China. *Advances in Atmospheric Sciences*, 36, 1171-1187.

680 Liang, X., Lettenmaier, D. P., Wood, E. F., & Burges, S. J. (1994). A simple hydrologically based  
681 model of land surface water and energy fluxes for general circulation models. *Journal of*  
682 *Geophysical Research: Atmospheres*, 99(D7), 14415-14428.

683 Liang, X., & Xie, Z. (2003). Important factors in land-atmosphere interactions: surface runoff  
684 generations and interactions between surface and groundwater. *Global and Planetary Change*,  
685 38(1-2), 101-114.

686 Liu, X., Chen, F., Barlage, M., Zhou, G., & Niyogi, D. (2016). Noah-MP-Crop: Introducing  
687 dynamic crop growth in the Noah-MP land surface model. *Journal of Geophysical Research:*  
688 *Atmospheres*, 121(23), 13-953.

689 McDaniel, R., Liu, Y., Valayamkunnath, P., Barlage, M., Gochis, D., Cosgrove, B. A., & Flowers,  
690 T. (2020, December). Moisture condition impact and seasonality of National Water Model  
691 performance under different runoff-infiltration partitioning schemes. In *AGU Fall Meeting*  
692 *Abstracts (Vol. 2020, pp. H111-0028)*.

693 Miguez-Macho, G., Fan, Y., Weaver, C. P., Walko, R., & Robock, A. (2007). Incorporating water  
694 table dynamics in climate modeling: 2. Formulation, validation, and soil moisture  
695 simulation. *Journal of Geophysical Research: Atmospheres*, 112(D13).

696 Nie, W., Kumar, S. V., Arsenault, K. R., Peters-Lidard, C. D., Mladenova, I. E., Bergaoui, K., ...  
697 & Navari, M. (2022). Towards effective drought monitoring in the Middle East and North  
698 Africa (MENA) region: implications from assimilating leaf area index and soil moisture into  
699 the Noah-MP land surface model for Morocco. *Hydrology and Earth System Sciences*, 26(9),  
700 2365-2386.

701 Niu, G.-Y., and Z.-L. Yang (2004), The effects of canopy processes on snow surface energy and  
702 mass balances, *J. Geophys. Res.*, 109, D23111, doi:10.1029/2004JD004884.

703 Niu, G.-Y., Z.-L. Yang, R. E. Dickinson, and L. E. Gulden (2005), A simple TOPMODEL-based  
704 runoff parameterization (SIMTOP) for use in global climate models, *J. Geophys. Res.*, 110,  
705 D21106, doi:10.1029/2005JD006111.

706 Niu, G.-Y., and Z.-L. Yang (2006), Effects of frozen soil on snowmelt run-off and soil water  
707 storage at a continental scale, *J. Hydrometeorol.*, 7, 937–952, doi:10.1175/JHM538.1.

708 Niu, G.-Y., Z.-L. Yang, R. E. Dickinson, L. E. Gulden, and H. Su (2007), Development of a simple  
709 groundwater model for use in climate models and evaluation with Gravity Recovery and  
710 Climate Experiment data, *J. Geophys. Res.*, 112, D07103, doi:10.1029/2006JD007522.

711 Niu, G.-Y., Yang, Z.-L., Mitchell, K. E., Chen, F., Ek, M. B., Barlage, M., et al. (2011). The  
712 community Noah land surface model with mul-  
713 tiparameterization options (Noah-MP): 1.  
714 Model description and evaluation with local-scale measurements. *Journal of Geophysical  
715 Research*, 116, D12109. <https://doi.org/10.1029/2010JD015139>

716 Niu, G. Y., Fang, Y. H., Chang, L. L., Jin, J., Yuan, H., & Zeng, X. (2020). Enhancing the Noah-  
717 MP ecosystem response to droughts with an explicit representation of plant water storage  
718 supplied by dynamic root water uptake. *Journal of Advances in Modeling Earth  
719 Systems*, 12(11), e2020MS002062.

720 Oleson, K. W., et al. (2004), Technical description of the Community Land Model (CLM), NCAR  
721 Tech. Note NCAR/TN-461+STR, 174 pp., Natl. Cent. for Atmos. Res., Boulder, Colo.  
722 (Available at [www.cgd.ucar.edu/tss/clm/distribution/clm3.0/index.html](http://www.cgd.ucar.edu/tss/clm/distribution/clm3.0/index.html).)

723 Patel, P., Jamshidi, S., Nadimpalli, R., Aliaga, D. G., Mills, G., Chen, F., ... & Niyogi, D. (2022).  
724 Modeling Large-Scale Heatwave by Incorporating Enhanced Urban Representation. *Journal of  
725 Geophysical Research: Atmospheres*, 127(2), e2021JD035316.

726 Sakaguchi, K., & Zeng, X. (2009). Effects of soil wetness, plant litter, and under-canopy  
727 atmospheric stability on ground evaporation in the Community Land Model (CLM3. 5). *Journal  
728 of Geophysical Research: Atmospheres*, 114(D1).

729 Salamanca, F., Zhang, Y., Barlage, M., Chen, F., Mahalov, A., & Miao, S. (2018). Evaluation of  
730 the WRF-urban modeling system coupled to Noah and Noah-MP land surface models over a  
731 semiarid urban environment. *Journal of Geophysical Research: Atmospheres*, 123(5), 2387-  
732 2408.

733 Saxton, K. E., & Rawls, W. J. (2006). Soil water characteristic estimates by texture and organic  
734 matter for hydrologic solutions. *Soil science society of America Journal*, 70(5), 1569-1578.

735 Sellers, P. J. (1985), Canopy reflectance, photosynthesis and transpiration, *Int. J. Remote Sens.*, 6,  
736 1335–1372, doi:10.1080/01431168508948283.

737 Sellers, P. J., M. D. Heiser, and F. G. Hall (1992), Relations between surface conductance and  
738 spectral vegetation indices at intermediate (100 m<sup>2</sup> to 15 km<sup>2</sup>) length scales, *J. Geophys. Res.*,  
739 97, 19,033–19,059, doi:10.1029/92JD01096.

740 Schaake, J. C., V. I. Koren, Q.-Y. Duan, K. E. Mitchell, and F. Chen (1996), Simple water balance  
741 model for estimating runoff at different spatial and temporal scales, *J. Geophys. Res.*, 101,  
742 7461–7475, doi:10.1029/95JD02892.

743 Suzuki, K., & Zupanski, M. (2018). Uncertainty in solid precipitation and snow depth prediction  
744 for Siberia using the Noah and Noah-MP land surface models. *Frontiers of Earth Science*, 12,  
672-682.



745 Valayamkunnath, P., Chen, F., Barlage, M. J., Gochis, D. J., Franz, K. J., & Cosgrove, B. A. (2021,  
746 January). Impact of Agriculture Management Practices on the National Water Model Simulated  
747 Streamflow. In 101st American Meteorological Society Annual Meeting. AMS.

748 Valayamkunnath, P., Gochis, D. J., Chen, F., Barlage, M., & Franz, K. J. (2022). Modeling the  
749 hydrologic influence of subsurface tile drainage using the National Water Model. *Water*  
750 *Resources Research*, 58(4), e2021WR031242.

751 Verseghy, D. L. (1991), CLASS-A Canadian land surface scheme for GCMS: I. Soil model, *Int. J.*  
752 *Climatol.*, 11, 111–133, doi:10.1002/joc.3370110202.

753 Wang, P., Niu, G. Y., Fang, Y. H., Wu, R. J., Yu, J. J., Yuan, G. F., ... & Scott, R. L. (2018).  
754 Implementing dynamic root optimization in Noah-MP for simulating phreatophytic root water  
755 uptake. *Water Resources Research*, 54(3), 1560-1575.

756 Wang, W., Yang, K., Zhao, L., Zheng, Z., Lu, H., Mamtimin, A., ... & Moore, J. C. (2020).  
757 Characterizing surface albedo of shallow fresh snow and its importance for snow ablation on  
758 the interior of the Tibetan Plateau. *Journal of Hydrometeorology*, 21(4), 815-827.

759 Wang, W., He, C., Moore, J., Wang, G., & Niu, G. Y. (2022). Physics-Based Narrowband Optical  
760 Parameters for Snow Albedo Simulation in Climate Models. *Journal of Advances in Modeling*  
761 *Earth Systems*, 14(1), e2020MS002431.

762 Wang, Y. H., Broxton, P., Fang, Y., Behrangi, A., Barlage, M., Zeng, X., & Niu, G. Y. (2019). A  
763 wet-bulb temperature-based rain-snow partitioning scheme improves snowpack prediction over  
764 the drier western United States. *Geophysical Research Letters*, 46(23), 13825-13835.

765 Warrach-Sagi, K., J. Ingwersen, T. Schwitalla, C. Troost, J. Aurbacher, L. Jach, T. Berger, T.  
766 Streck, and V. Wulfmeyer, 2022: Noah-MP with the generic crop growth model Gecros in the  
767 WRF model: Effects of dynamic crop growth on land-atmosphere interaction. *J Geophys Res-*  
768 *Atmos*, 127(14), e2022JD036518.DOI:10.1029/2022JD036518

769 Wrzesien, M. L., Pavelsky, T. M., Kapnick, S. B., Durand, M. T., & Painter, T. H. (2015).  
770 Evaluation of snow cover fraction for regional climate simulations in the S ierra N  
771 evada. *International Journal of Climatology*, 35(9), 2472-2484.

772 Wu, W. Y., Yang, Z. L., & Barlage, M. (2021). The Impact of Noah-MP Physical  
773 Parameterizations on Modeling Water Availability during Droughts in the Texas–Gulf  
774 Region. *Journal of Hydrometeorology*, 22(5), 1221-1233.

775 Xia, Y., K. Mitchell, M. Ek, J. Sheffield, B. Cosgrove, E. Wood, L. Luo, C. Alonge, H. Wei, J.  
776 Meng, B. Livneh, D. Lettenmaier, V. Koren, Q. Duan, K. Mo, Y. Fan, and D. Mocko (2012).  
777 Continental-scale water and energy flux analysis and validation for the North American Land  
778 Data Assimilation System project phase 2 (NLDAS-2): 1. Intercomparison and application of  
779 model products. *J. Geophys. Res.*, 117, D03109, doi:10.1029/2011JD016048

780 Xu, T., Chen, F., He, X., Barlage, M., Zhang, Z., Liu, S., & He, X. (2021). Improve the  
781 performance of the noah-MP-crop model by jointly assimilating soil moisture and vegetation  
782 phenology data. *Journal of Advances in Modeling Earth Systems*, 13(7), e2020MS002394.

783 Xu, X., Chen, F., Shen, S., Miao, S., Barlage, M., Guo, W., & Mahalov, A. (2018). Using WRF-  
784 urban to assess summertime air conditioning electric loads and their impacts on urban weather  
785 in Beijing. *Journal of Geophysical Research: Atmospheres*, 123(5), 2475-2490.

786 Xue, Y., P. J. Sellers, J. L. Kinter, and J. Shukla (1991), A simplified bio- sphere model for global  
787 climate studies, *J. Clim.*, 4, 345–364, doi:10.1175/1520-  
788 0442(1991)004<0345:ASBMFG>2.0.CO;2.

789 Yang, Z.-L., and R. E. Dickinson (1996), Description of the Biosphere- Atmosphere Transfer  
790 Scheme (BATS) for the soil moisture workshop and evaluation of its performance, *Global*  
791 *Planet. Change*, 13, 117–134, doi:10.1016/0921-8181(95)00041-0.

792 Yang, Z. L., Niu, G. Y., Mitchell, K. E., Chen, F., Ek, M. B., Barlage, M., ... & Xia, Y. (2011).  
793 The community Noah land surface model with multiparameterization options (Noah-MP): 2.  
794 Evaluation over global river basins. *Journal of Geophysical Research: Atmospheres*, 116(D12).

795 Yen, Y. C. (1965). Effective thermal conductivity and water vapor diffusivity of naturally  
796 compacted snow. *Journal of Geophysical Research*, 70(8), 1821-1825.

797 Yen, Y. C. (1981). Review of thermal properties of snow, ice, and sea ice (Vol. 81, No. 10). US  
798 Army, Corps of Engineers, Cold Regions Research and Engineering Laboratory.

799 Zhang, G., Chen, F., & Gan, Y. (2016). Assessing uncertainties in the Noah-MP ensemble  
800 simulations of a cropland site during the Tibet Joint International Cooperation program field  
801 campaign. *Journal of Geophysical Research: Atmospheres*, 121, 9576–9596. [https://doi.](https://doi.org/10.1002/2016JD024928)  
802 [org/10.1002/2016JD024928](https://doi.org/10.1002/2016JD024928)

803 Zhang, X. Y., Jin, J., Zeng, X., Hawkins, C. P., Neto, A. A., & Niu, G. Y. (2022a). The  
804 compensatory CO2 fertilization and stomatal closure effects on runoff projection from 2016–  
805 2099 in the western United States. *Water Resources Research*, 58(1), e2021WR030046.

806 Zhang, X., Xie, Z., Ma, Z., Barron-Gafford, G. A., Scott, R. L., & Niu, G. Y. (202b). A Microbial-  
807 Explicit Soil Organic Carbon Decomposition Model (MESDM): Development and Testing at a  
808 Semiarid Grassland Site. *Journal of Advances in Modeling Earth Systems*, 14(1),  
809 e2021MS002485.

810 Zhang, Z., Barlage, M., Chen, F., Li, Y., Helgason, W., Xu, X., ... & Li, Z. (2020). Joint modeling  
811 of crop and irrigation in the central United States using the Noah-MP land surface  
812 model. *Journal of Advances in Modeling Earth Systems*, 12(7), e2020MS002159.

813 Zhang, Z., Chen, F., Barlage, M., Bortolotti, L. E., Famiglietti, J., Li, Z., ... & Li, Y. (2022).  
814 Cooling Effects Revealed by Modeling of Wetlands and Land-Atmosphere Interactions. *Water*  
815 *Resources Research*, 58(3), e2021WR030573.

816 Zhang, Z., Li, Y., Chen, F., Harder, P., Helgason, W., Famiglietti, J., Valayamkunnath, P., He, C.,  
817 and Li, Z.: Developing Spring Wheat in the Noah-MP LSM (v4.4) for Growing Season  
818 Dynamics and Responses to Temperature Stress, *Geosci. Model Dev. Discuss.* [preprint],  
819 <https://doi.org/10.5194/gmd-2022-311>, in review, 2023.

820 Zhuo, L., Dai, Q., Han, D., Chen, N., & Zhao, B. (2019). Assessment of simulated soil moisture  
821 from WRF Noah, Noah-MP, and CLM land surface schemes for landslide hazard  
822 application. *Hydrology and Earth System Sciences*, 23(10), 4199-4218.

823 Zonato, A., Martilli, A., Gutierrez, E., Chen, F., He, C., Barlage, M., ... & Giovannini, L. (2021).  
824 Exploring the effects of rooftop mitigation strategies on urban temperatures and energy  
825 consumption. *Journal of Geophysical Research: Atmospheres*, 126(21), e2021JD035002.  
826